North Sea Transnational Grid

A better way to integrate large scale Offshore Wind Power

Summary report

J. Pierik, E. Wiggelinkhuizen, F. Nieuwenhout, M. van Hout **(ECN)**

R. Teixeira Pinto, S. Rodrigues, P. Bauer **(TUD EPP)**

M. Gibescu, A. van der Meer, A. Ciupuliga, M. Ndreko, B. Rawn **(TUD EPS)**

January 2014
Project number: EOS LT 08019

ECN-E - - 14-004

Contents

Introduction

A huge amount of wind power, 30-60 GW, is foreseen in the northern part of the North Sea. These wind farms have to be connected to the national grids of five different countries in a flexible and economical way. Individual connection is straightforward but for several reasons possibly not the best choice. A high capacity North Sea Transnational Grid connecting wind farms to the national grids and at the same time connecting the national grids together, may well be a better solution for reasons of energy efficiency, availability, controllability, lower costs and the possibility to trade/exchange electricity .

The objective of the North Sea Transnational Grid project is to determine the best solution (modular, flexible, most cost effective) for a high capacity transnational offshore grid, connecting all future wind farms in the northern part of the North Sea to the Netherlands, UK, Norway, Denmark and Germany. Different technical solutions for a Transnational Grid will be investigated. For the most promising solution a multi-terminal converter controller will be developed and tested. A second objective is to determine the effects of the Transnational Grid on the national grids, in which the operating strategy of the Transnational Grid will be developed to regulate power exchange correctly and avoid congestion. Moreover, the effect of the Transnational Grid on national grid stability will be investigated. The costs, benefits, policies and regulations related to realization of the North Sea Transnational Grid will also be investigated and compared to alternative scenarios.

This report summarizes the main results of the project by describing the results of the main work packages. More detailed information can be found in the technical reports prepared for each work packages. The final section contains a list of these reports and the papers prepared in the NSTG project. The reports and the public papers can be downloaded from the NSTG website: www.nstg-project.nl

This project was financially supported by the Ministry of Economic Affairs under the Energie Onderzoek Subsidie - Lange Termijn (EOS-LT) programme, executed by AgentschapNL.

1

Management Summary

This section gives a short overview of the main results.

Technical and economic evaluation of different solutions Transnational Grid and alternatives

This work package started with the determination of the possible locations and development stages for a total amount of wind power of 52.8 GW in the North Sea. Next, the cost of transporting energy have been evaluated for two scenarios by modelling in EeFarm. In the first scenario an offshore grid with integrated wind and trade connections is studied (wind connected to trade ring). This is based on DC connections and advanced AC-DC technology. In the second scenario, wind farms are individually connected to the onshore grid and is based on conventional AC technology. Based on the currently available price estimates, the integrated scenario based on DC connections is the best solution. This option is further examined in the next work packages.

Transnational Grid multi-terminal operation and control

The main objective was the development of a control strategy for the multi-terminal DC grid of scenario 1 in the previous work package. Existing control methods have been investigated and qualified. By applying linear control theory and operational optimization, a novel control strategy was developed: Distributed Voltage Control (DVC). This control method gives lower losses and better controllability. To test the control method, dynamic models of the multi-terminal DC grid and connected wind farms were developed. Simulation showed that the DVC method worked according to design.

Multi-terminal converter testing on RTDS

A small multi-terminal DC grid was built in the laboratory. It consists of three controlled Voltage Source Converters (VSC), resistors and inductors. One of the converters was operated as an offshore wind farm through control by a real time digital simulator (RTDS: OPAL-RT). The RTDS also executed the DVC. Measurements showed that the dynamic models used to design the controller were accurate and that the DVC worked as expected. The method is easily extended to grids with more converters.

Optimization
Apart from application of optimization in the novel Distributed Voltage Control method, multi-objective optimization was applied in two case studies: finding the best transmission system design and optimizing the power flow and social welfare of a meshed offshore multi-terminal DC grid.

Grid integration: planning, congestion and stability
The first part of this work package identifies the effect of the North Sea offshore grid on the congestion and N-1 security of the onshore grid, in particular for the Netherlands. This is based on market simulation (unit commitment and economic dispatch considering inter-area constraints). Different offshore topologies, similar to the scenarios in other work packages, have been compared. Trade connections between hubs belonging to the same country resulted in rather low usage resulting in a preference for a radial instead of a ring structure. Power flow calculations identified the main bottlenecks for the Dutch transmission grid.

Secondly, the influence of an integrated North Sea Transnational Grid based on VSC technology on the dynamics of the onshore AC grid was investigated. A dynamic model of the power system of continental Europe was used in combination with transmission simpler models of the British and Nordic system. The transient stability study investigated three-phase short circuit faults. A U-shaped offshore DC grid gave slightly better results than point-to-point connections. Simulation of a second type of instability, rotor angle oscillations, showed that the transnational DC grid potentially has a mitigating effect.

Costs, benefits, regulations and market aspects
This work package compared the economic benefits of the base case: wind and trade not integrated (no ring) to two NSTG scenarios: wind and trade integrated (full ring) and a full ring equivalent (equivalent transport capacity on land). The scenarios were implemented in the COMPETES market model covering most Western European countries. It was concluded that for Europe as a whole the investment in the full ring and the full ring equivalent have a positive NPV (net present value) compared to the base case. There are differences in benefits between the individual countries however.

International collaboration (IEA Annex 25)
The NSTG project contributed to the IEA Annex 25: Design and Operation of Power Systems with Large Amounts of Wind Power.

Dissemination of results
The reports of the work packages and the open source papers prepared in the project are available at the project web site. The project will be closed with a presentation on the work package results and a final discussion with advisory group and interested third parties.

Main results
The main results of the NSTG project are:

- Steady state models for the connection of a large amount of offshore wind combined with trade connections in the North Sea;
- Evaluation of scenarios for the connection of a large amount of offshore wind and trade based on different technologies (electrical parameters, losses, cost of transport of energy);

- Improved wind farm dynamic models, with emphasis on control and operation of the electrical system;
- A novel controller (DVC) for a multi-terminal DC grid connecting offshore wind energy based on linear control strategy and operational optimization;
- Demonstration of DVC in a small three converter laboratory grid with one converter simulating wind power using an RTDS;
- Validation of dynamic models of the voltage source converters;
- Optimization of power flow in a multi-terminal DC network;
- Multi-objective optimization of transmission system design for offshore wind energy;
- Consequences of the North Sea offshore grid on the operation and security of the onshore grid;
- Consequences of the North Sea offshore grid on the dynamics of the onshore grid (faults and rotor angle stability);
- Evaluation of a base case and two NSTG scenarios in the COMPETES market model of Western Europe;
- Detailed technical reports with all results;
- Two PHD-thesis;
- A large number of conference and journal papers.

This project shows that the proposed solution for the integration of a large amount of wind power and a transnational trade grid is promising from an economic point of view. A technical problem inhibiting the introduction, namely the control of a multi-terminal DC grid, was solved in this project.

2

WP2: Technical and economic evaluation of different solutions Transnational Grid

Work Package 2 of the North Sea Transnational Grid (NSTG) project covers the steady state and economic evaluation of different solutions for the North Sea Transnational Grid. This will be based on EeFarm electrical and economic calculations for the different technical options and scenarios. The EeFarm program calculates electrical variables, losses, not produced power due to failure, investment costs and the transport costs averaged over the economic life time of the systems (LTC).

In the first part of Work Package 2, the possible locations and development phases of wind power in the North Sea have been determined, see figure 1. The total amount of wind power will be 52800 MW, divided over 48 wind farms of 1100 MW each. This choice was based on the maximum size of a single DC connection. This wind farm and connection rating is also used as base case in the other work packages of the NSTG project (WP6 and WP7). The reason for this choice is that the largest available VSC-HVDC connection results in the lowest relative investment costs (Euro per installed MW).

Two scenario's will be investigated:

- North Sea Transnational Grid with interconnected wind power and trade connections (NSTG integrated scenario);
- Individual wind power connections to shore (AC connected) and a separate transnational DC trade grid (AC-DC separated scenario).

Figure 1: North Sea Transnational Grid and wind farm locations (photo: NASA)

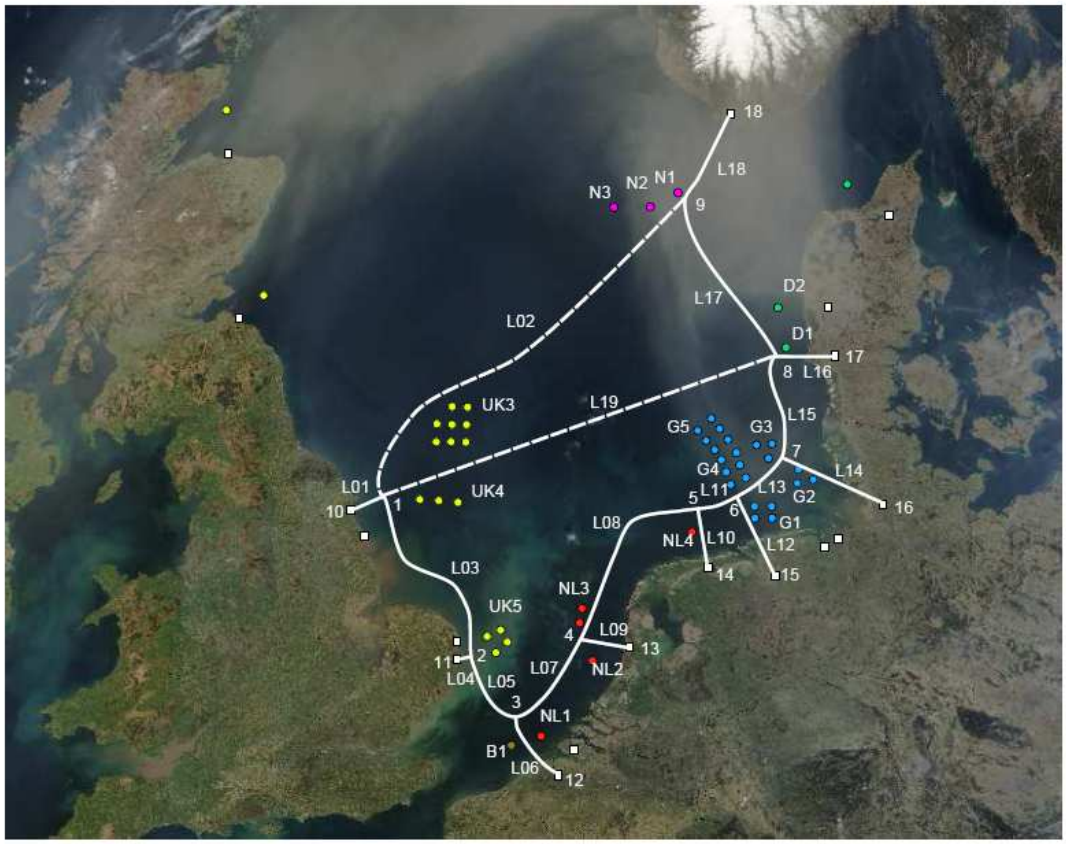

Both scenarios consist of the same cable routes. In scenario 2 a number of extra connections are required to connect the ring shaped trade grid to the onshore grid since the wind farm connections are not used for this purpose. The scenarios are compared on a level of individual connections per development phase as well as in total. Both scenarios were developed in ten stages or phases with an approximately equal increase in wind power per phase.

The scenarios are compared in three ways: wind power connections only, trade connections only and the total of wind and trade together. The scenarios are compared by calculating the average levelized transport cost of the system, in other words the average LTC per connection and phase.

Table 1: Scenario 1 and 2: Wind connections only

Scenario 1: Wind DC	Phase 1	Phase 2	Phase 3	Phase 4	Phase 5
number of WF	6	10	14	19	23
Inv (MEuro)	4816.2	7968.1	11215.7	15339.5	18638.5
LTC ave (Euro/kWh)	0.01270	0.01256	0.01263	0.01273	0.01277
Scenario 2: Wind AC	Phase 1	Phase 2	Phase 3	Phase 4	Phase 5
number of WF	6	10	14	19	23
Inv (MEuro)	5171.2	8394.9	11534.8	16641.1	20927.4
LTC ave (Euro/kWh)	0.01339	0.01301	0.01275	0.01361	0.01418

Scenario 1: Wind DC	Phase 6	Phase 7	Phase 8	Phase 9	Phase 10
number of WF	30	35	40	44	48
Inv (MEuro)	24470.6	28623.8	32975.6	36451.1	39941.3
LTC ave (Euro/kWh)	0.01286	0.01289	0.01300	0.01306	0.01312
Scenario 2: Wind AC	Phase 6	Phase 7	Phase 8	Phase 9	Phase 10
number of WF	30	35	40	44	48
Inv (MEuro)	28661.6	34653.5	41391.0	46255.3	51697.6
LTC ave (Euro/kWh)	0.01493	0.01550	0.01626	0.01654	0.01698

Table 1 compares only the wind connection investment costs and the average LTC per phase for both scenarios. The LTC for the wind connections is based on the transported wind power only, trade is not taken into account. The investment costs and average LTCs are higher for the AC connected scenario than for the DC scenario. **Figure 2** A shows that the difference between the LTC values for wind only increases after phase 3.

The AC solution requires a relatively larger number of parallel connections, while the DC solution is based on a single connection. The losses for the 10 shortest AC connections are below the DC system losses and for the remaining 6 above the DC losses. Due to the relatively larger number of parallel connections, the not produced power due to failure is negligible for the AC solutions (about 0.2%). For the DC connection including the two converters this is about 1.8-2.5%. This does not reverse the investment cost disadvantage of the AC system however, as shown by the LTC values.

Figure 2: Average Levelized Transport Costs: Wind only (A) and Wind plus Trade (B) for both scenarios

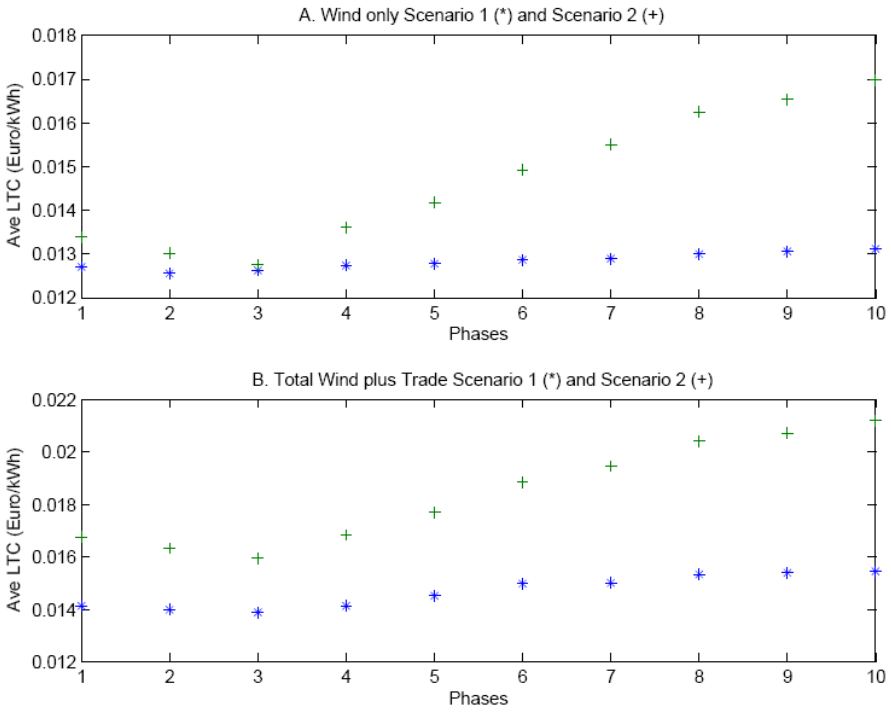

Table 2: Trade connections only in Scenario 1 and 2: Scenario 2 requires both Ring and Trade to Shore

Scenario 1 and 2: Ring (Trade)	Phase 1	Phase 2	Phase 3	Phase 4	Phase 5
number of trade connections	7	7	9	11	14
Inv (MEuro)	1286.8	1286.8	1455.9	1970.7	3110.4
LTC ave (Euro/kWh)	0.00143	0.00143	0.00126	0.00139	0.00174
Scenario 2: Trade to Shore	Phase 1	Phase 2	Phase 3	Phase 4	Phase 5
number of trade connections to shore	4	6	8	10	12
Inv (MEuro)	985.3	1433.9	1963.3	2308.9	2698.6
LTC ave (Euro/kWh)	0.00195	0.00189	0.00194	0.00183	0.00178

Scenario 1 and 2: Ring (Trade)	Phase 6	Phase 7	Phase 8	Phase 9	Phase 10
number of trade connections	17	17	19	19	19
Inv (MEuro)	4559.0	4559.0	5588.5	5588.5	5588.5
LTC ave (Euro/kWh)	0.00212	0.00212	0.00233	0.00233	0.00233
Scenario 2: Trade to Shore	Phase 6	Phase 7	Phase 8	Phase 9	Phase 10
number of trade connections to shore	14	15	16	16	17
Inv (MEuro)	3183.9	3492.7	3706.0	3706.0	4051.5
LTC ave (Euro/kWh)	0.00180	0.00184	0.00183	0.00183	0.00189

Table 2 list the trade connection total investment cost and average LTC per phase for both scenarios. The ring connections are present in both scenarios. The trade to shore connections are only required for scenario 2. Since scenario 2 requires additional DC connections to shore, it requires the highest investment and results in the highest average

LTC per connection: the sum of the ring and trade to shore values. The LTC for a trade connection is based on permanent use at maximum power.

Scenario 2 has the relative advantage of full availability for trade of the connections to shore. In scenario 1, the power trade may be limited by the transported wind power over a connection to shore. This effect is reduced by the relatively large number of wind farm connections (48 in phase 10) to the number of transnational connections (19 in phase 10).

Figure 2 B shows the total LTC values of wind and trade in both scenarios. Compared to **Figure 2** A, the increase represents the cost of transporting traded power between countries assuming full use of all trade connections all the time in both scenarios. The LTC increases most in scenario 2 due to the additional connections to shore.

Table 3: Scenario 1 and Scenario 2 Wind and Trade Total

Scenario 1: Wind DC + Trade	Phase 1	Phase 2	Phase 3	Phase 4	Phase 5
Inv (MEuro)	6103.0	9255.0	12671.6	17310.1	21748.9
LTC ave (Euro/kWh)	0.01413	0.01398	0.01388	0.01413	0.01452
Scenario 2: Wind AC + Trade	Phase 1	Phase 2	Phase 3	Phase 4	Phase 5
Inv (MEuro)	7443.3	11115.6	14954.0	20920.6	26736.4
LTC ave (Euro/kWh)	0.01676	0.01633	0.01595	0.01683	0.01770

Scenario 1: Wind DC + Trade	Phase 6	Phase 7	Phase 8	Phase 9	Phase 10
Inv (MEuro)	29029.6	33182.8	38564.0	42039.5	45529.7
LTC ave (Euro/kWh)	0.01498	0.01501	0.01533	0.01539	0.01545
Scenario 2: Wind AC + Trade	Phase 6	Phase 7	Phase 8	Phase 9	Phase 10
Inv (MEuro)	36404.5	42705.2	50685.4	55549.7	61337.6
LTC ave (Euro/kWh)	0.01884	0.01946	0.02042	0.02071	0.02120

The results for wind and trade together, presented in **Table 3**, again show that the investment costs play a dominant role in the comparison of the scenarios. The transport cost follow the trend in the investment costs. Combining wind and trade in a single average LTC per phase, the differences between scenario 1 and 2 increase to the detriment of scenario 2.

The critical factor determining the results in this study was the investment cost of the systems. The manufacturer supplied component prices in the EeFarm database were compared to recent ETSO-E data and for the DC system partly updated in an upward direction. When comparing AC and DC options, there appears to be more room for technical improvement (for instance loss reduction) and subsequent price reduction (due to increasing experience in design and operation) for the DC option.

3

WP 3a: Wind Farm Dynamic Models

3.1 Introduction

This chapter summarizes a non-linear dynamic wind farm model and its simulation in the MTDC grid, which belongs to WP3a. The wind farm model has been integrated with a MTDC grid model, see **Figure 3**, and a simplified AC-grid model to simulate and test the complete system and the optimal power flow method "Distributed Voltage Control" under various operating conditions, which are described in more detail under WP3b and WP4.

Figure 3: Topology of the modeled MTDC grid

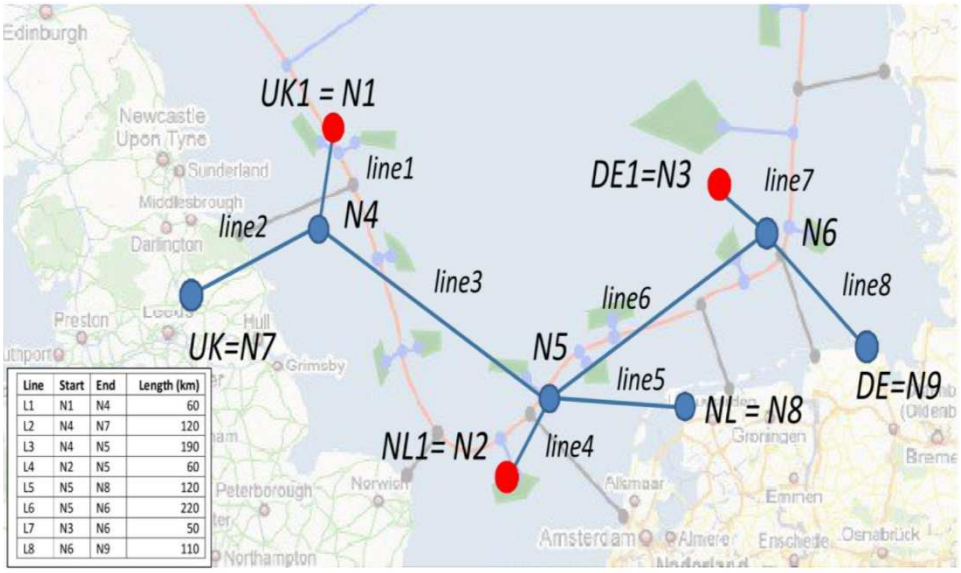

Line	Start	End	Length (km)
L1	N1	N4	60
L2	N4	N7	120
L3	N4	N5	190
L4	N2	N5	60
L5	N5	N8	120
L6	N5	N6	220
L7	N3	N6	50
L8	N6	N9	110

3.2 Technology selection

The wind farm model consists of variable speed pitch control turbines with a permanent magnet generator and full-rated voltage source converter. The wind farm collection grid is aggregated to a single string of wind turbines or even to a single wind turbine connected to an AC bus through a single AC cable. The wind farm is connected to the DC grid via an AC/DC converter, for which a Voltage Source Converter (VSC) in chosen.
The models and the controls of the wind farms, the HVDC converters and the passive components are described with their implementation in Matlab/Simulink®. The model assumes symmetrical voltages and does not contain switching elements, harmonic filters and protection systems. However the dynamics and physical limitations relevant for the grid stability are modeled.

Figure 4 Wind farm technologies and grid connection options

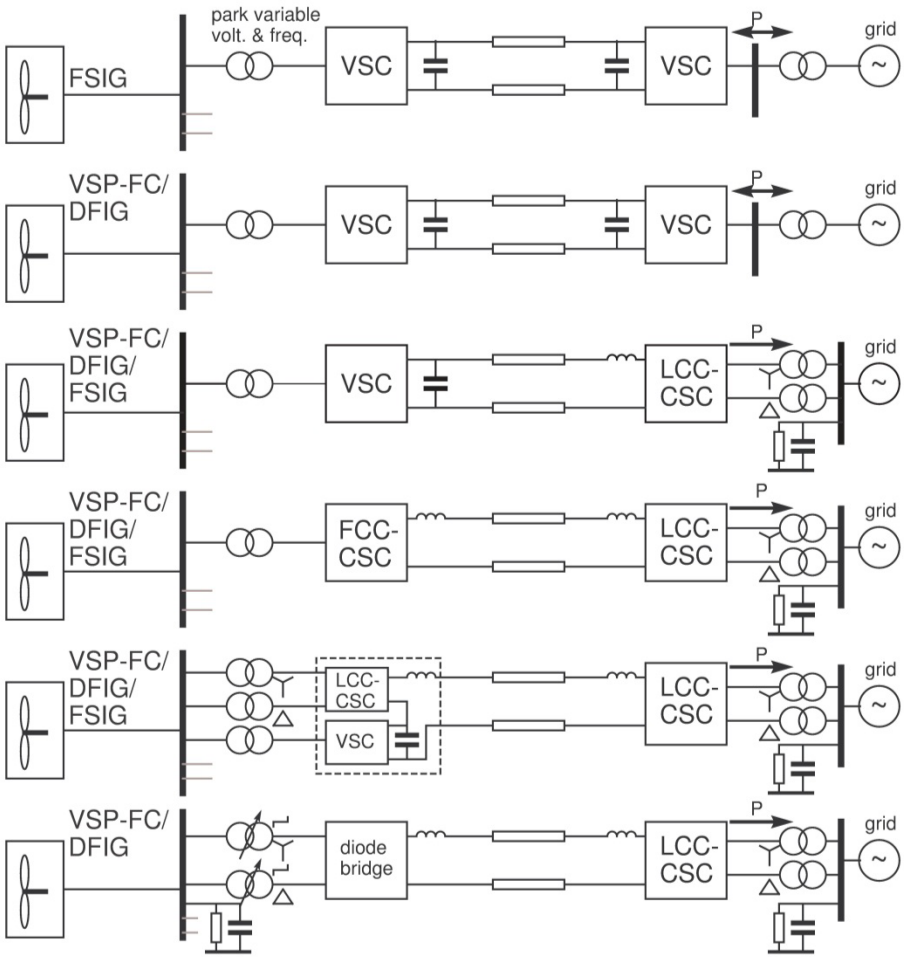

Converters
Different technology combinations of wind turbines and converters have been presented and discussed, cf. **Figure 4**. Among others, combining VSC converters with Forced Commutated Current Source Converters in theory offers advantages for handling DC-faults. As the power flow control of FC-CSC will be analogue to VSC control only VSCs are considered.

Wind turbine types
For the wind turbine type a Variable Speed Pitch-controlled type with full-rated converter is chosen because this type shows good control capabilities, which are especially needed for balancing the power in the MTDC grid. The Fixed speed types without converter have poor control capabilities and need additional equipment to preserve power quality. DFIG wind turbines connected via HVDC are supposed to behave similar to wind turbines with full-rated converters, except for short-circuit current and asymmetrical faults. However, the AC-voltage in the wind farm is controlled by the HVDC converters, therefore asymmetrical faults are less likely and also the short-circuit current contribution is less relevant than with an AC grid connection.

Control design
Under normal conditions all available power from the wind farm is converted to DC, so the power flow control should be performed by the grid-connected converter stations in the MTDC network. For VSC stations this is equivalent to controlling the DC voltage.

The wind farm VSC is set supply the AC voltage and frequency according to fixed setpoint values. In case of power imbalance in the DC network, or more specific, DC over-voltage, the WF power output should be reduced almost instantly. Because reducing the generator torque needs some time and because of limitations of the converters, chopper-controlled braking resistors are needed to dissipate the excess power. The WF power reduction can be accomplished in different ways, depending on the type and design of the VSC station and the wind farm.

The wind turbine model is based on an existing 6MW demo turbine including the controller. The wind turbine grid-side VSC control has been adapted to operate in combination with a VSC, in particular the reactive current injection during voltage dips. The VSC control settings in the MTDC grid have been copied from the settings derived in WP3b. The controller optimisation using the linearized models has not yet been implemented in this model.

3.3 Model description

3.3.1 Modeling assumptions

The models only consider symmetrical AC-voltages and currents, represented as dynamic phasors. The passive component models consist of lumped frequency-dependent network elements. Converters are modelled as non-switching and lossless, only a low-pass filter is included to represent the switching delay. PLLs for estimating the grid voltage angle and rotor flux position, is represented by low-pass filters.

3.3.2 MTDC grid model

For simplicity, each wind farm node and each onshore node in the small MTDC grid represents a single voltage-source converter (VSC) station of 1GW. Also the nominal power of each of the wind farms is chosen as 1GW, see **Figure 5**, so that the capacity is sufficient to transport all wind power to the nearest country. Trading of offshore wind power or onshore generated power to other countries via line3 and line6 in **Figure 3** is possible up to the available capacities of the VSC stations of the three countries.

Figure 5 Components of the modelled MTDC grid (DE nodes)

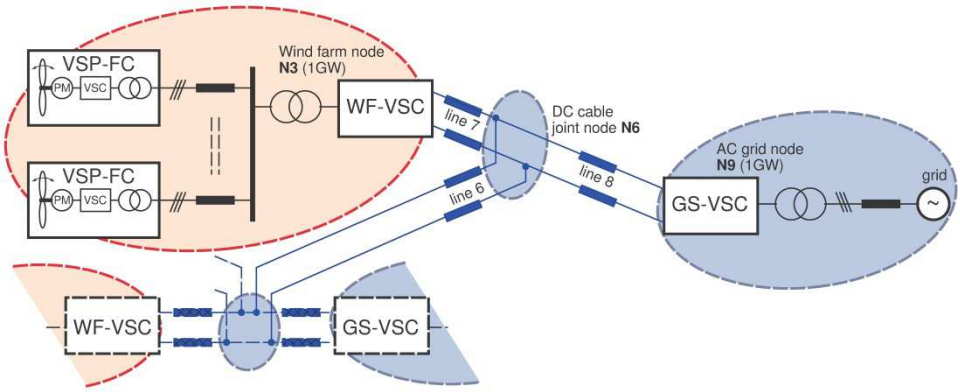

The rated power of each of the wind farms and of each converter is chosen equal to 1GW. The nominal interconnection voltage is chosen equal to 640kV (cable pair of +/-320kV), as this is the highest voltage for which offshore cables are currently available, so that transmission losses over longer distances are minimized.
In the model of the MTDC network each DC cable connection is represented by a single PI-section. At each node half the capacitance of the connected cables is added to the VSC station capacitance. The voltage is assumed to be perfectly balanced.
Two AC grids (NL and DE) are modelled as an infinite bus behind a short circuit series impedance, while the UK AC grid is modelled as a single synchronous generator with a series line impedance and a shunt resistance to model a 3-phase fault. The short-circuit power is chosen equal to 5000 MVA.

MTDC operation
The wind farm converter (WF-VSC) operates as rectifier and controls the wind farm AC voltage to a fixed reference, while the power production is determined by the wind farm. The grid side converters (GS-VSC) together control the power flow in the DC-network such that the DC node voltages and line currents stay within safe operating limits and electrical losses are minimized. For this power flow control a new method, called Distributed Voltage Control (DVC), which is developed at TU-Delft, is applied. Compared to other possible control methods it shows good dynamic response as well as good scalability, i.e. that it is applicable for complex networks, and fail-safe operation.

3.3.3 Wind Farm

The upper scheme in **Figure 6**shows the wind farm electrical layout in which each five wind turbines are connected to a string feeder. Because of the large size of the wind farm the model it should be simplified, which is done by aggregating components, as shown in the lower scheme. The collection grid is represented by a single cable, the power generated by a single string is upscaled with a factor of N_{par}, which is the number of parallel strings, and the wind turbines are represented by a single VSC. The power input of this VSC $P_{e\text{-}aggr}(t)$ is generated by combining three wind turbine model outputs, as shown in **Figure 7**.

Figure 6 Wind farm component aggregation

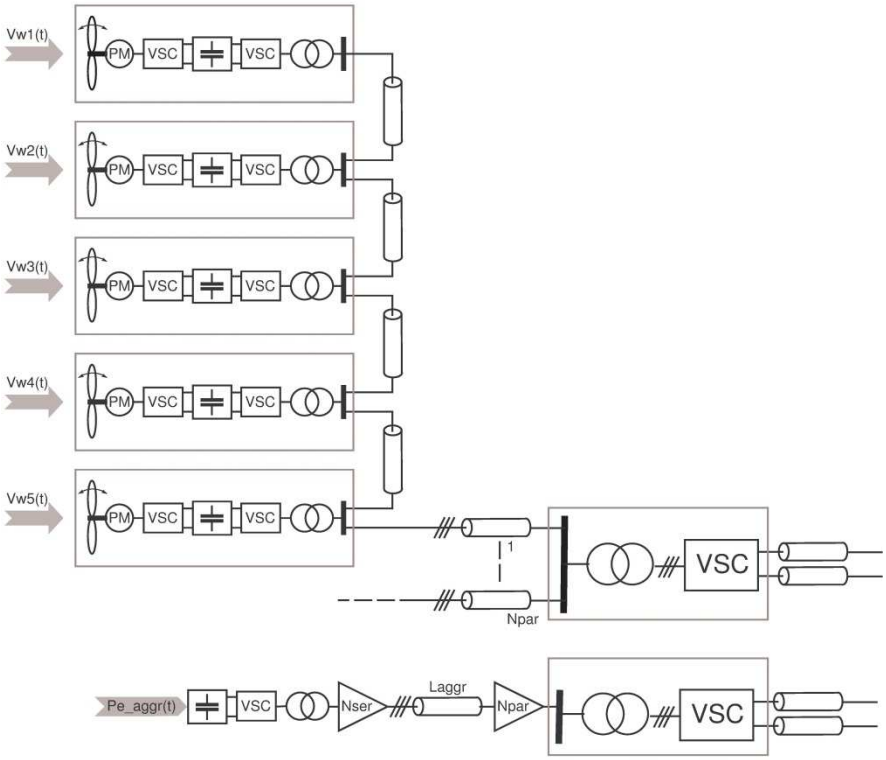

Figure 7 Wind farm output power smoothing

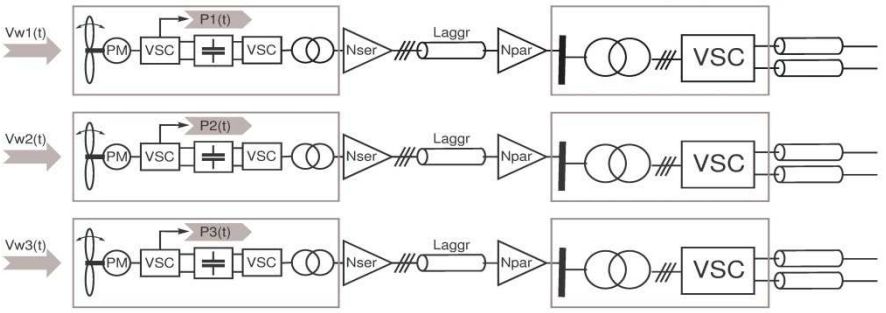

Depending on the position of a wind turbine in the farm a different power output series is selected and a delay time, inversely proportional to the wind speed, is added. The wind speed deficits in the wind farm due to wake effects are only estimates, as more accurate calculations are complicated and need detailed information of the turbines, the wind farm layout and the atmospheric conditions. Depending on the simulation case different undisturbed wind speed series are applied. The method leads to a sufficiently low correlation between the power outputs, which leads to a reduction of the variance in the power spectrum of $\sqrt{N}$ compared to a single wind turbine output.

3.4 Converter model

The VSC models used in the wind turbine and in the MTDC grid have a similar structure, cf. similar **Figure 8**, although the operational settings differ, depending on the station type. (WT-VSC, WF-VSC of GS_VSC), as shown in **Figure 9**.

Figure 8: Simplified VSC block scheme

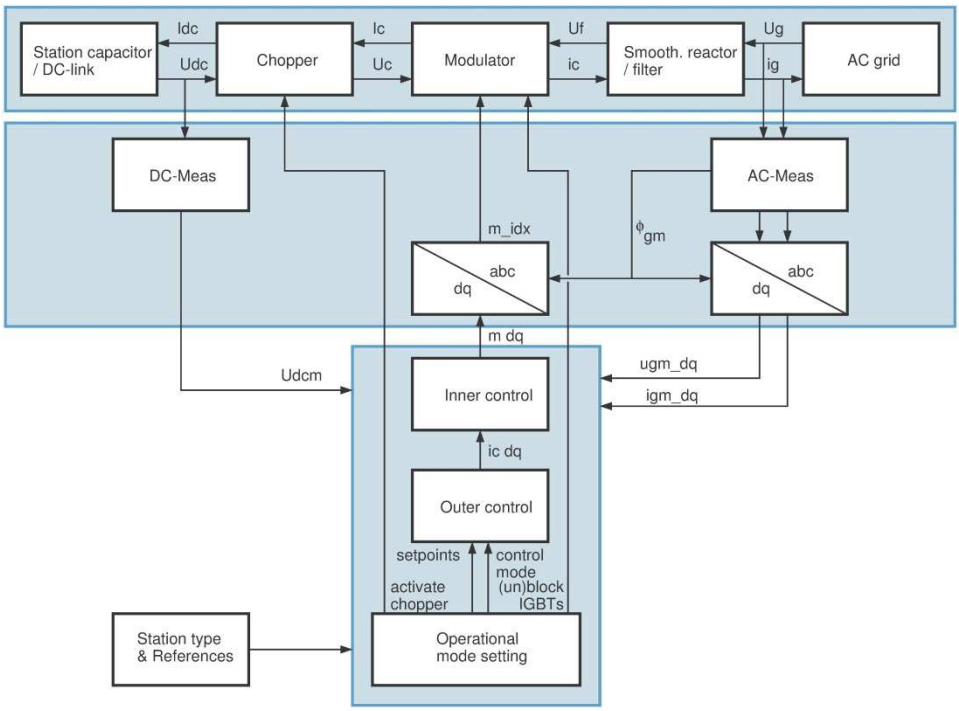

For instance, during an AC-grid voltage dip the HVDC-GSC prioritizes the reactive power for voltage support. Also, an external active power limitation is implemented, e.g. for grid frequency support, while for the WT external power control is implemented by lowering the aerodynamic power through the rotor speed angular speed setpoint. For the wind turbine generator-side VSC the vector control reference angle is the estimates rotor flux rather than the estimated voltage angle. Details of the control design are described in the NSTG WP3a report.

Figure 9: VSC operational mode settings

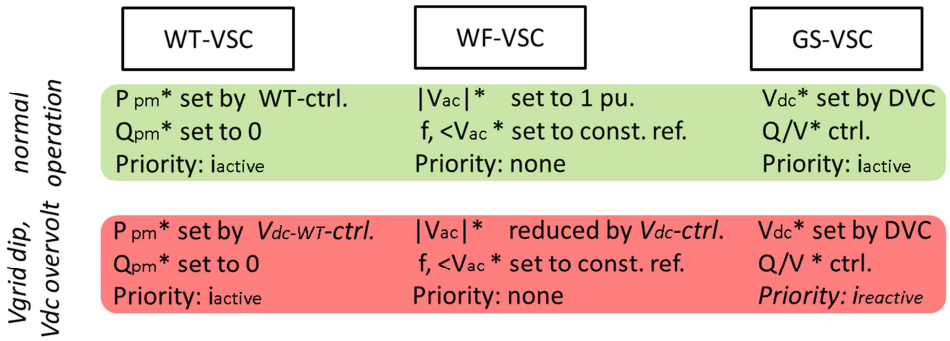

3.5 Simulations

For a number of cases, cf. **Table 4** under different operational conditions simulations have been performed for the MTDC grid, including the dynamic wind farm models.

Table 4: Description of the analysed case studies

	Case Study	Description
1. Start-up procedures	1a. MTDC start-up	During the start-up procedure, the MTDC system voltage is charged from zero to the rated system voltage value by the GS-VSC terminals.
2. Normal operation	2a. Priority	Priority is given to the country where the wind energy is being produced, i.e. all the power goes to the rightful country; while there is no energy trade.
	2b. Proportional sharing	The sum of all the energy being produced by the OWFs is equally divided amongst all the countries through energy trade via the MTDC network.
	2c. Reversed power flow	The power flow of the German node is reversed. At first the power is flowing from the MTDC network into Germany and, in a later stage, this power flow is reversed.
3. Wind curtailment	3a. Low-wind scenario	The MTDC system behaviour is analysed during wind curtailment in a scenario where the wind energy generation is low.
	3b. High-wind scenario	The MTDC system behaviour is analysed during wind curtailment in a scenario where the wind energy generation is high.
4. AC-contingency	4a. Low-wind scenario	The MTDC system behaviour is analysed during an ac-fault at the UK node in a scenario where the wind energy generation is low. In this case study the MTDC network is N-1 secure.
	4b. High-wind scenario	The MTDC system behaviour is analysed during an ac-fault at the UK node in a scenario where the wind energy generation is high. In this case it cannot be guaranteed that the MTDC network is N-1 secure.

As an example some results are presented in **Figure 10**, **Figure 11** and **Figure 12**

Figure 10: Simulation results of selected cases for normal operation

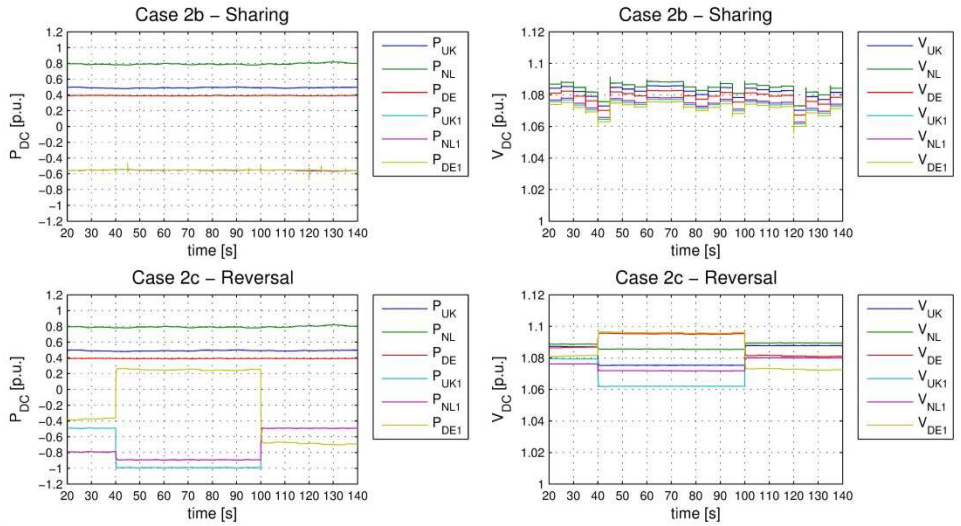

Figure 11 Simulation results of selected cases for wind curtailment

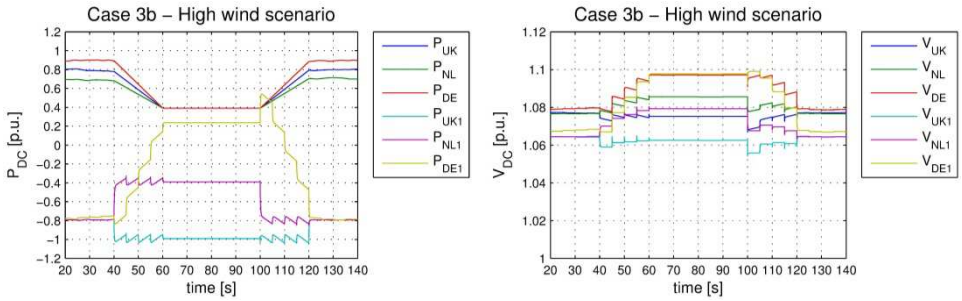

Figure 12 Simulation results of selected cases for AC-contingencies

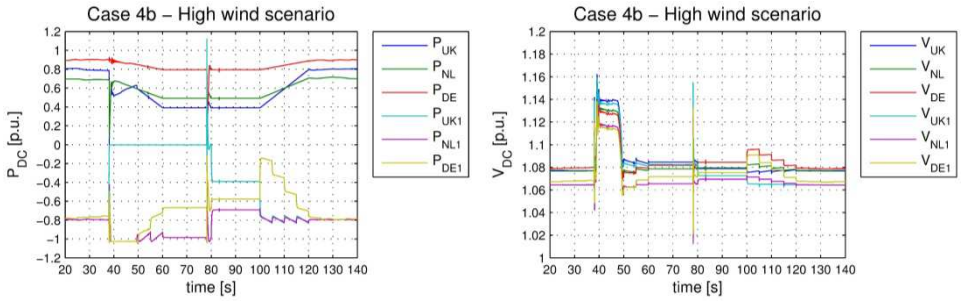

3.5.1 Discussion

The results from case 2b show that the produced wind power is equally shared between the three connected countries, while 2c shows good dynamic response to an abrupt power set-point change.
Case e 3b shows that because of the changing power flow demands from the TSOs the power flow to the UK is saturated. Still the DVC power control remains power balance.
Case 4b shows that the MTDC grid keeps in operation during an AC-grid fault at the UK side between t=40-80 sec. The power of the WFs after fault clearance is set to ramp up slowly after the fault clearance. The fault clearance leads to power oscillations because the AC-grid voltage needs to stabilize, although the IGBTs are blocked until the voltage is considered stable.

3.6 Conclusions

As part of WP3 of the NSTG project different technical solutions for a transnational grid have been evaluated. The selected technology for the NSTG is based on Voltage Source Converters and variable speed pitch turbines with full-rated VSC converter.
The wind farm model and been integrated with the MTDC model and the DVC power flow control method has been applied successfully in this simulation model, both under normal operation and for a number of events, such as optimal DC-power flow under certain restrictions and dynamic events such as AC-voltage dips and black-starts.

In order to make the next step towards implementation, the modeling of the wind farms in combination with MTDC networks can be improved in many ways. The most relevant aspects are considered to be:

- Communication delays and limitations to the accuracy of the wind farm and MTDC grid SCADA system, both for power and voltage measurements and for setting wind farm power levels and VSC DC-voltage levels.
- Simulate high wind speed cut-out and the best use of wind power prediction for the MTDC grid operation.
- Modeling of converter losses and other HVDC converter technologies. i.e. multi-level VSCs
- Detailed cable modeling, both electro-magnetic and thermal
- Study the combination of storage systems connected to the MTDC grid and the consequences for its design and operation.

Also the DVC method can be developed further to handle these practical limitations.
For more complex MTDC networks solutions to preserve power flow control in mazed networks can be elaborated, e.g. by applying parallel grids in order to ensure onshore grid stability without the need for numerous DC-breakers.

4

WP3b: Transnational Grid Operation and Control

In work package 3b, the control strategies aiming at flexibility and modularity of the Transnational Grid were investigated. By applying linear control theory and optimization algorithms, a novel control strategy was designed using the developed dynamic models of the high-voltage dc voltage-source converters (VSC-HVDC) and of the multi-terminal dc (MTDC) network. The controllability of the Transnational Grid is then realised by control of the voltage source converters incorporated into the MTDC system.

The main objectives of work package 3b were:

- build the nonlinear dynamic model of the VSC-HVDC converters and of the Transnational Grid;
- inventory of VSC control with emphasis on multi-terminal connections;
- development of a voltage source converter controller for bi-directional multi-terminal operation.

4.1 Modular Model of the North Sea Transnational Grid (NSTG)

A future NSTG will be built in a modular way, therefore it is only natural that the models used to describe the system should also be modular in nature. Dynamic models of future large offshore multi-terminal dc networks are needed for assessment of the overall system behavior, during normal and fault conditions, to study the interactions between the offshore wind farms, the power electronic converters and other dc equipment, but also for control designing purposes.

Modular dynamic models allow highly complex systems to be divided into smaller sub-modules. To model large offshore transnational grids, the approach used in the NSTG project was to derive the equations driving the dynamic models of the most important system modules, namely: the offshore wind farms, the VSC-HVDC stations and the multi-terminal dc grid.

With this modular approach, it is possible to study the dynamic behavior of the complete North Sea Transnational Grid. **Figure 13** displays a modular representation of MTDC networks for integration of offshore wind energy with the different system components and the interaction between them.

Figure 13: Modular representation of offshore MTDC networks

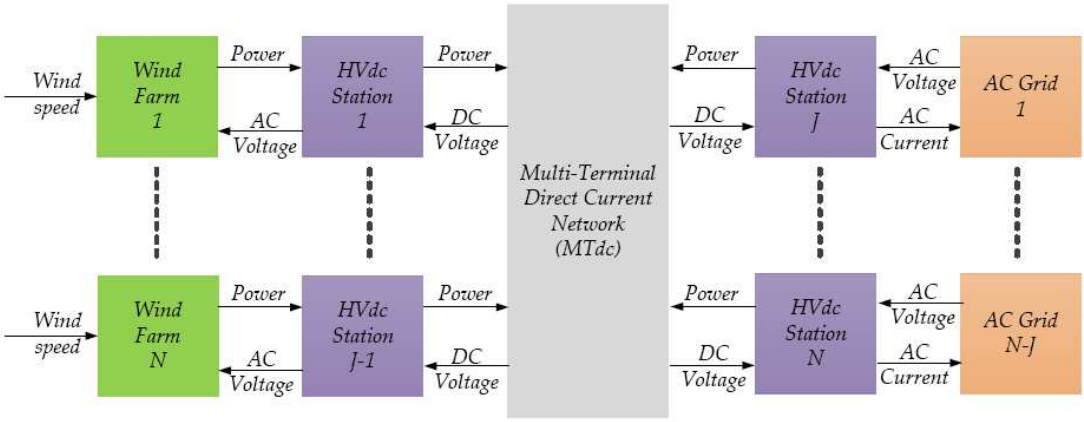

4.1.1 Multi-terminal DC Network Model

The transmission lines in VSC-HVDC can be either overhead lines (OHL) or via dc underground or submarine cables.
As power flow reversal in the VSC-HVDC does not require the inversion of the direct voltage polarity, the dc cables can be designed to use extruded polymeric insulation as a substitute to the conventional oil-impregnated paper insulation. This results in lighter and more flexible cables, easier and quicker to install. These dc cables can withstand high forces and repeated stresses making them suitable for severe deep-water conditions.

Present rated voltages on use in VSC-HVDC transmission schemes, with underground or submarine cables, are up to +/- 320kV in bipolar configurations.
In the MTDC network model each dc cable is represented by a pi-section circuit. The next figure shows a generic representation of a MTDC network for offshore wind energy integration.

Figure 14: Generic representation of a MTDC grid

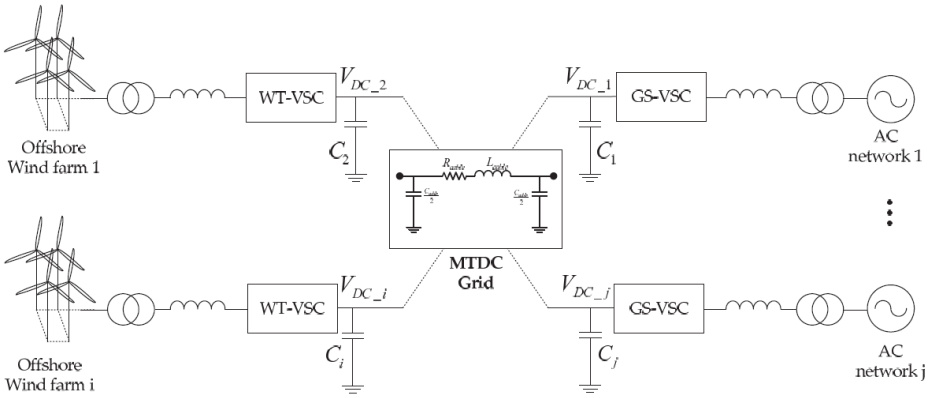

Figure 15: Single-line diagram of a VSC-HVDC transmission station.

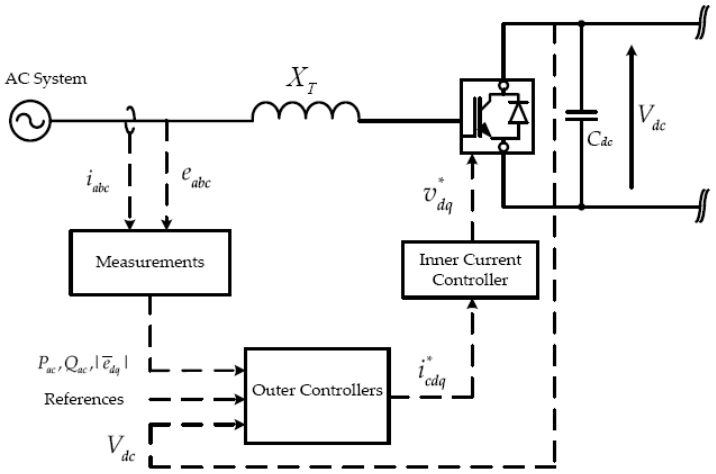

4.1.2 VSC-HVDC Model

The single-line representation of a VSC-HVDC transmission station with its control structure is depicted in **Figure 15**.
Due to the switching behavior of the several IGBTs constituting a VSC, the dynamic equations describing the converter operation are discontinuous and complex to solve. One way to deal with complex power electronic converter modelling is to employ averaged dynamic models, whose main purpose is to simplify the converter analysis while still allowing enough details to understand its dynamics and to develop control strategies.

The VSC model developed in the NSTG project is an averaged lossless model. In an averaged model, the closed-loop bandwidth of the VSC current controller is usually kept at least 5 times lower than the switching frequency. Therefore, the converter switching behavior can be neglected when evaluating its dynamic response inside MTDC networks. The developed VSC-HVDC station model is modular and contains several modules: viz.: a phase reactor, the converter model, the station capacitor, an inner current controller, and the outer

controllers. **Figure 16** (a) depicts the signal-flow inside the complete VSC-HVDC model, whereas **Figure 16** (b) explains the converter model block.

Figure 16: VSC-HVDC system modular dynamic models

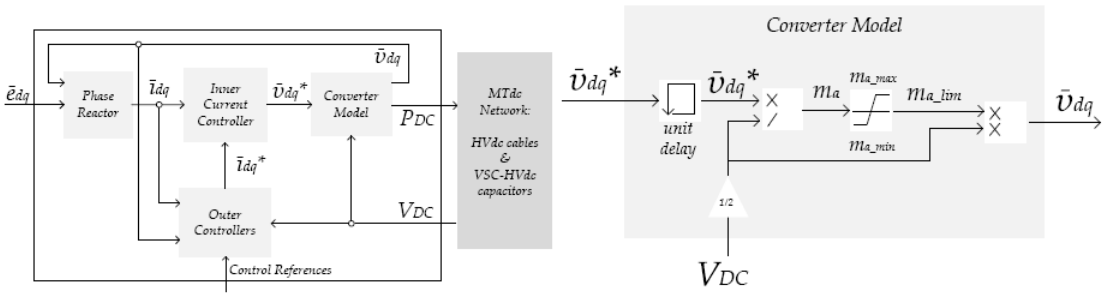

(a) Complete VSC-HVDC station (b) Voltage-source converter model

4.1.3 VSC-HVDC Control

A VSC can control the active and the reactive power exchanged with the ac transmission system in an independent way. The goal of the VSC controller is to set the amplitude, the angle and the frequency of the converter phase voltages. There are two main control strategies to achieve that objective: direct control and vector control. In the NSTG project focus was given to vector control, as this is the most employed VSC control structure.

In vector control, the converter currents and the three-phase voltages are transformed to the rotating direct-quadrature frame, which will be then synchronized with the ac network voltage by means of a phase-locked loop (PLL). The control system determines the converter voltage reference in the *dq* frame via an inner-current controller, and this signal is fed back to the converter after it is re-transformed to the three-phase *abc*.

4.2 MTDC Network Control

Inside a MTdc network, direct voltage control is certainly one of the most important tasks given to VSC-HVdc stations. A well-controlled direct voltage on a HVdc grid requires a balanced power flow between all the interconnected nodes. In point-to-point HVdc transmission systems the control is typically arranged so that one terminal controls the dc-link voltage while the other operates in current -or power - regulation mode. To guarantee a secure and reliable grid operation, future large multi-terminal dc networks will require instead that the responsibility of controlling the direct voltage inside the system is shared by more than one VSC-HVdc station. A suitable control strategy for large MTdc networks will have fast dynamic behaviour, high flexibility(ability to control the network power flow), high expandability(the ability to control large dc grids), and if possible, low communication requirements.
In the NSTG project the four most common direct voltage control strategies for sharing the direct voltage control in MTDC networks were analyzed, namely: droop control, ratio

control, priority control and voltage margin method control . A short description of each control strategy is given next.

1. Droop Control: Works similarly to the droop control implemented in traditional ac systems, where the load dependent frequency variation is used as an input signal for the control system to adjust the generated power to meet demand. In MTdc networks the control employs the droop mechanism to regulate the direct voltage within the system by adjusting the converter current so that power balance is guaranteed.
2. Ratio Control: is a modification of the droop control to address the difficulty of steering the power flow in the network. In this control strategy, a power ratio is established between two or more dc system voltage controlling stations and the converters will then share the generated power accordingly to the desired ratio set by the system TSO.
3. Priority Control: one VSC terminal will have precedence over the other terminals for the power being input in the MTdc network. In the case of the North Sea Transnational grid this translates into precedence over the power produced by the offshore wind farms. This control strategy is accomplished by combination of two different direct voltage controllers: PI and proportional (or droop) controllers.
4. Voltage Margin Method Control: This control method was first proposed by Tokiwa et al. in 1993 and, in 1999, Nakajima and Irokawa to control a 3-terminal back-to-back MVdc scheme in Japan. In the VMM, each converter station is given a marginally offset direct voltage reference, called margin. Similarly to the current margin method for CSC-MTdc networks, the voltage margin is defined as the direct voltage reference difference between the VSC terminals.

4.3 The Distributed Voltage Controller

All the analysed MTDC network control methods suffered from different issues, such as limited power flow control, difficult expandability to larger MTdc networks or poor dynamic performance. Therefore, a novel control strategy was developed inside the NSTG project. The control strategy named Distributed Voltage Control (DVC), focuses on controlling the VSC-HVdc terminals direct voltages to control the power flow inside MTdc networks.

The DVC strategy, depicted in **Figure 17**, work as follows: at first, the DVC receives the power production at the offshore wind farms (OWFs). Then, a distributed dc load flow algorithm is run to obtain a first solution for the optimal power flow (OPF) algorithm. The OPF problem can be solved via any optimization method, such as a steepest gradient method or via a genetic algorithm, such as the one developed in the work package 5 of the NSTG project. The DVC can therefore be used to minimize the MTDC network losses, or maximize its social welfare, or even have a combination of goals in a multi-objective optimization.

Figure 17: Flowchart diagram of the Distributed Voltage Control strategy

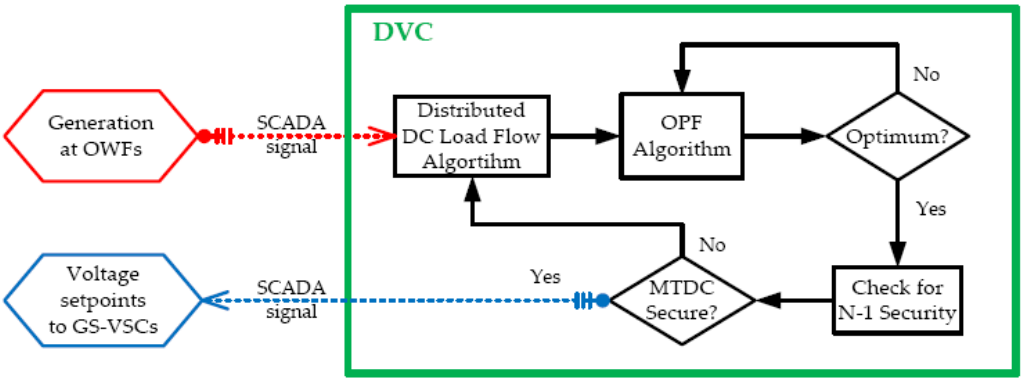

The constraints and specific parameters for the OPF algorithm are set by the transmission system operator (TSO). Next, the OPF solution is checked for N-1 security. On that point, the GS-VSCs are made slack nodes, i.e. they control the direct voltage at their respective nodes to the value defined by the OPF algorithm. The distributed DC load-flow algorithm then runs N load-flow scenarios, with one dc node defective at a time, to check whether the MTDC network is N-1 secure for the obtained power-flow scenario. In the end, the DVC sends the direct voltage set-points to the onshore converters (GS-VSCs).
As it relies only on a central optimal power flow solution, SCADA communication systems can be used to gather the necessary information just as for power plant control in ac networks. The advantage of the DVC strategy is that, in practice, a desired load-flow scenario can be kept fixed for a certain amount of time (e.g., 15 min control cycle). Hence, in essence, a fast communication link with the TSO is also not needed. Nevertheless, it is necessary to be able to send the voltage references to the onshore converter stations once every control cycle.
Therefore, the DVC strategy is readily expandable to larger MTdc networks, and more nodes controlling the network direct voltage will add more flexibility to the method. In the DVC strategy, network nodes which are not directly connected to generating plants work as slack nodes controlling the MTdc network voltage. This increases the system resilience against ac faults, and it additionally provides a higher flexibility, i.e. ability to control the power flow inside the system, by finding a solution to an optimal power flow problem.

A total of three publications, using the dynamic models developed in the NSTG project, demonstrated that the DVC strategy is capable of reliably and safely controlling the power flow in large MTdc networks with good dynamic performance.

5

WP4 : Multi-terminal DC Network Testing

In work package 4 (WP4), the results of WP3 were tested by scaled experiments. For this purpose, a small multi-terminal dc network, with 3 nodes, was built and tested at Technical University of Delft. The experiments were first run in a stand-alone way, and subsequently with the aid of an OPAL-RT real time digital simulator, where signals from a real offshore wind farm were recorded. The experiments also comprised a validation of the dynamic models of the voltage-source converters and of the distributed voltage control strategy. The main objectives in this work package were:

- Setting up the small scale multi-terminal converter system in the laboratory to test the operation and control strategies developed in WP3;
- Converter stand-alone measurements and converter model validation;
- Connection of the small scale multi-terminal converter to the RTDS and testing the operation and control;

5.1 VSC Model Validation

The dynamic models and controls developed in WP3 were tested in a 5-kVA VSC in the laboratory of the Electrical Sustainable Energy Department of Delft University of Technology. **Figure 18** displays a picture of the voltage-source converter and real-time controller used during the experiments, whereas the most important VSC component values are given in **Table 5**.

For the validation of the VSC dynamic model, the converter was connected to the 380-voltage ac grid as a static synchronous compensator (STATCOM), as shown in **Figure 18**(b). During the test, all the VSC controllers presented in WP3 were tested.

Figure 18: Laboratory setup for validating the VSC models

(a) VSC cabinet, real-time controller, and host PC.

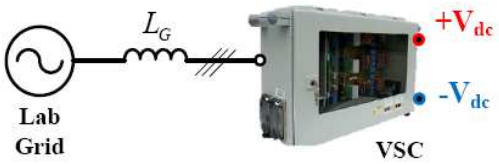

(b) VSC as a static synchronous compensator.

Table 5: Rated parameters of the VSC used in the laboratory experiments

Parameter	Symbol	Value	Unit
VSC Rated Power	S_{vsc}	5000	VA
VSC ac-side Voltage	V_c	380	V
Grid-side Inductance	L_g	1.5	mH
Grid-side Resistance	R_g	0.2	Ω
Filter Capacitance	C_f	20	μF
Converter Inductance	L_c	1.5	mH
Converter Resistance	R_c	0.2	Ω
DC-Side Voltage	V_{dc}	700	V
DC-Side Capacitor	C_{dc}	500	μF

Figure 19(a) shows the VSC response to a step in the reactive power. The results are shown for the 5-kVA VSC (blue), the non-linear model (green), and the small-signal model (red line). A The positive value means the converter is absorbing reactive power from the lab ac grid. **Figure 19**(a) shows the VSC reactive power response is very fast (less than 100 ms) and that both the non-linear and the small-signal models agree with the laboratory measurements.

Figure 19(b) shows the VSC response to a step in the direct voltage reference. The direct voltage response is as fast as the reactive power one. The direct voltage results from the VSC large-signal model, and the measurements taken in the 5-kVA VSC show a very good agreement. However, the small-signal model, due to disregarded nonlinearities, does not correctly predict the small overshoots in the direct voltage.

Figure 19: Measurements obtained during the VSC model validation experiments

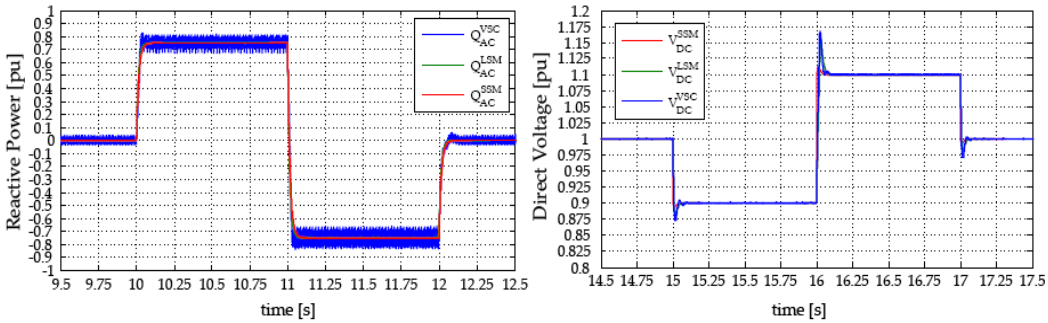

(a) Reactive power (b) Direct Voltage

5.2 Real Time Controller and Control Structure

All models to control the voltage-source converters in the low-voltage MTdc network were developed using Simulink. **Figure 20** shows the control communication structure and the developed control blocks. After a model is developed using Simulink, the models are then compiled in C/C++ and uploaded to the Target PC, which will control the operation of the voltage-source converters in real time. The PWM signals are calculated using the developed model and sent to an Ethernet switch which routes the signals to the respective converter. The converter switching frequency is 16kHz, thus the control algorithm step time was selected as 62.5 microseconds.

Figure 20: Communication structure of the experimental setup

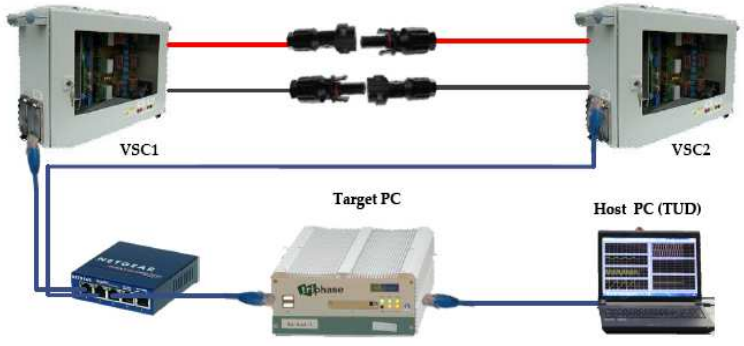

The converters operate with a controller (Target PC) which computes the control algorithms and transmits the PWM signals, in real-time, to the converters using an Ethernet communication protocol. The converters then send back the current and voltage measurements to the Target PC which forwards the information to the Host PC, closing the hardware-in-the-loop control structure.

Once a control step is finished, the converter measurements -- i.e. ac grid voltages and currents, converter currents and direct voltage -- are made available in the Simulink model via the *Grid coupling PM5F30C* block. As shown in **Figure 21**, the voltage-source converter

control is composed of the measurements block, the phase-locked loop *PLL* block, and the converter control *Cabinet Control* block.

5.3 MTDC Network Implementation

Three voltage-source converters were connected in a radial MTdc network as shown in Figure. The converters, VSC1, VSC2 and VSC3, are connect to each other via 4 mm2 LVdc cable. To improve safety, all equipments and cables were insulated and at the cable joints Multi-Contact MC4 connectors, rated for 20A currents and voltages up to 1000V, were used. The voltage-source converters employed in the low-voltage MTdc network setup are two-level converters whose mid-point of the dc bus is connected via a filter to the converter neutral at the grid side. Therefore, the MTdc network is formed by a symmetric monopole topology and its rated voltage is 700V or +/-350V.

Figure 21: Control structure of the voltage-source converters

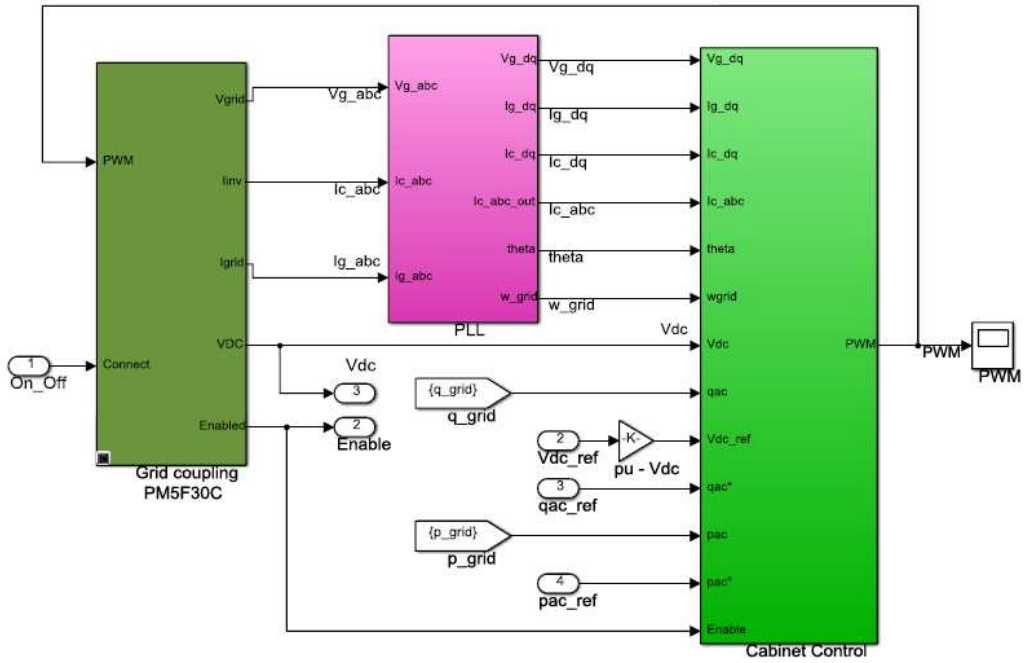

After understanding the operation of the MTdc network with three terminals, the low-voltage setup was used to validate the Distributed Voltage Control (DVC) strategy developed in this thesis. The final setup is displayed in **Figure 23**, which shows the Opal-RT real-time digital simulator, the Triphase real-time controller, the three voltage-source converters -- VSC1 to VSC3 -- and the resistance boxes used to emulate the three-terminal dc grid.

Figure 22: Layout of the low-voltage scaled-down MTdc network to be studied

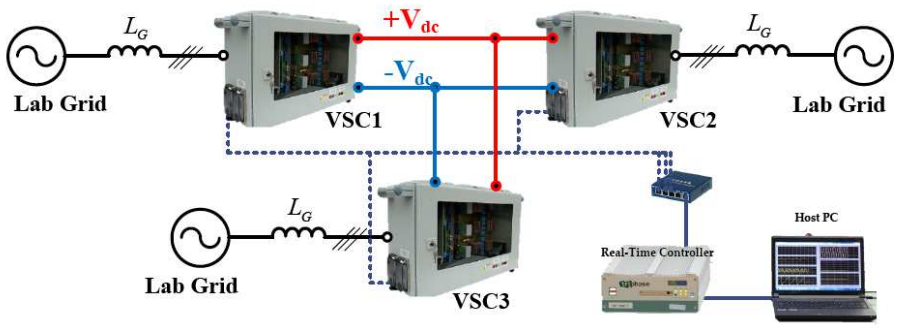

Figure 23: MTdc network for the validation of the Distributed Voltage Control strategy

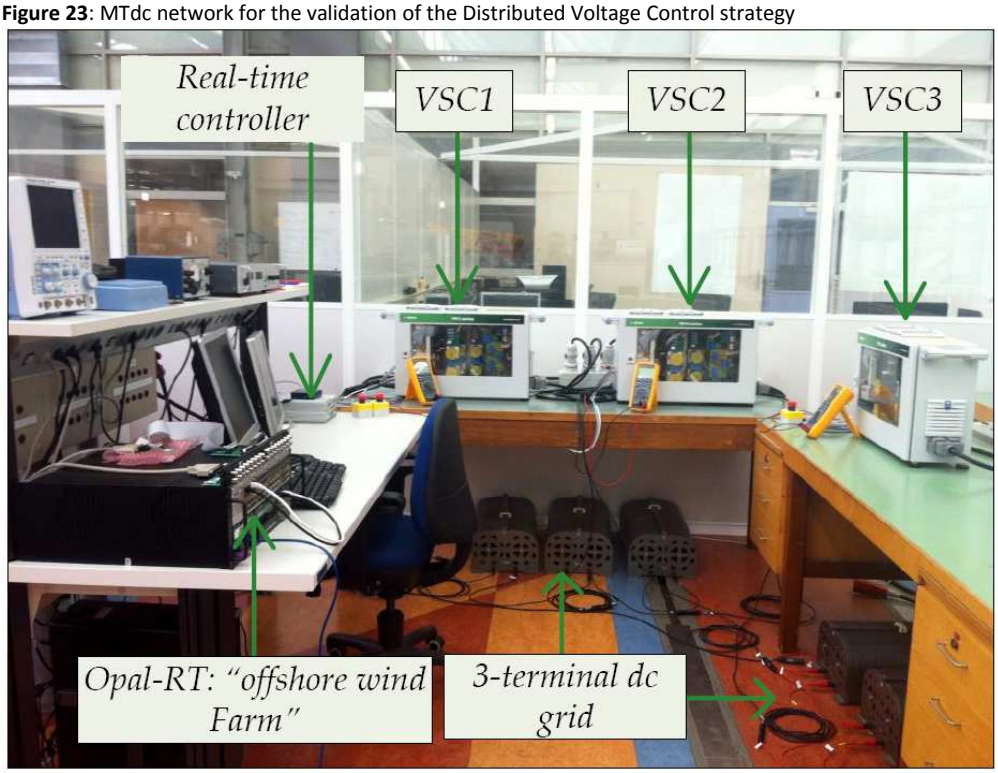

The experiments for the validation of the DVC strategy are explained next in three steps:

- the offshore wind farm implementation;
- the control strategy implementation in the real-time controller and;
- the experimental results.

5.3.1 OWF Implementation

To validate the developed control strategy, a power curve from a real offshore wind turbine was used. The wind turbine measurements came from the Dutch offshore wind farm in the North Sea, *Egmond aan Zee* (OWEZ).

The offshore wind farm, located circa 20 km from the Dutch coast and occupies an area of 27km^2, has a total installed capacity of 108MW and it comprises of 36 V90 wind turbines, rated at 3MW each, from Danish manufacturer Vestas Wind Systems A/S. **Figure 24**(a) shows the OWF power curve used in the DVC validation experiments. The power curves obtained from the OWEZ wind farm were for only one offshore wind turbine; hence, had a higher variability than what is expected from the aggregated power of the whole offshore wind farm. Therefore, the power curve shown in **Figure 24**(a) is the result of a filtering process to smooth the output power of a single turbine into that of the complete offshore wind farm.

During the experiments, the VSC3 was operated as the converter connected to the offshore wind farm. The active power reference for VSC3 came from an OPAL-RT real-time digital simulator. **Figure 24**(b), shows the OPAL-RT analog signal, representing the offshore wind farm power, being read by an oscilloscope, whereas **Figure 25** depicts the offshore wind farm signal flowchart.

Figure 24: Wind power signal from OPAL-RT real-time simulator used in the DVC strategy validation experiments

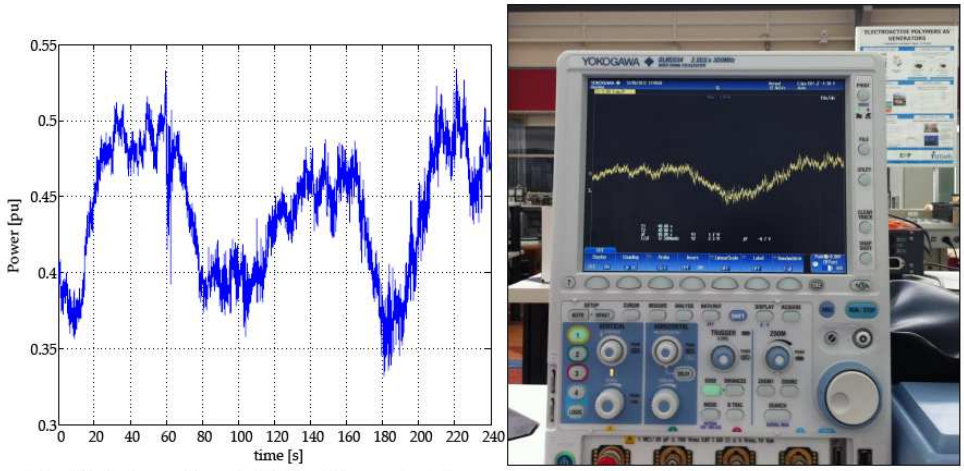

(a) Wind Power from OWEZ offshore wind farm (b) Wind Signal from OPAL-RT

First, the offshore wind farm signal was loaded into the OPAL-RT simulator. Secondly, the analog signal was given to a Beckhoff 16-bits differential analog-digital converter (ADC) module (EL3102). The nominal operational range of the ADC is limited to +/-10V, whereas the OPAL-RT analog output voltage can deliver up to +/-16V.
Although the input-filter limit frequency of the ADC is 5kHz, the signal sampling frequency was kept much lower, at 64Hz, which is the original sampling frequency of the OWEZ signal. After the offshore wind farm signal was converter from analog to digital, it was sent to the Triphase real-time controller, re-transformed from a voltage reading into a per unit value and given to VSC3 as an active power reference signal.

Figure 25: Flowchart of the offshore wind farm signal

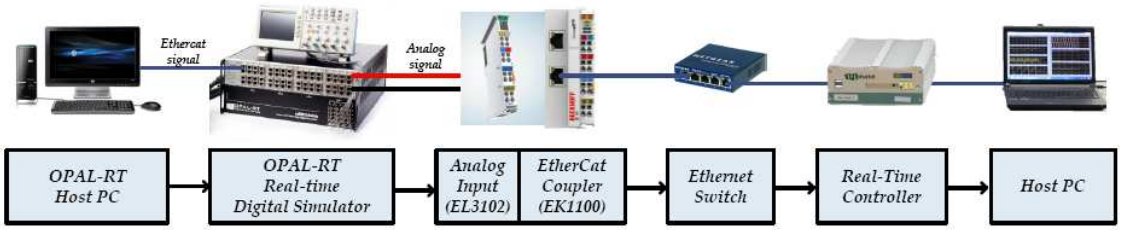

5.3.2 DVC Strategy Implementation

In the low-voltage MTdc network setup, the DVC strategy experimental implementation was realised using Matlab/Simulink Stateflow. **Figure 26** shows the Stateflow block which implemented the DVC strategy.

Figure 26: Matlab/Simulink Stateflow block with the implementation of the distributed voltage control strategy

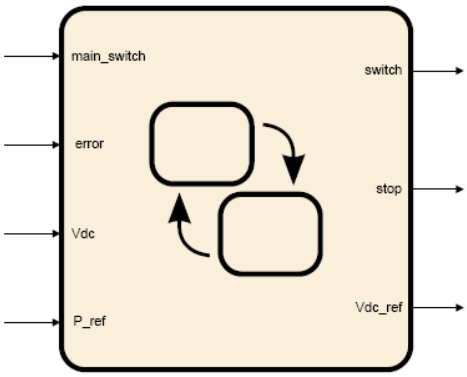

The DVC Stateflow block contains four inputs, which are needed for the optimal power flow procedure, and three outputs which are used to control the power flow in the MTdc network, by controlling the direct voltages of the VSC1 and VSC2 terminals. The first input *main_ switch* is used to commence the system operation. Upon initialization, all converters ac-side switches are set to zero, i.e. open, and all voltage references are set to 1pu. Five seconds after the *main_ switch* signal is set to 1, VSC1 starts up and tries to bring the MTdc network voltage to 1pu.
The status of a converter is read from the second input, the *error* signal (see **Figure 26**). If any of the converter fails during the start-up procedure, the system goes into a *STOP* state, which there are three in total, and operation is halted.

The third input *Vdc* signal -- are the direct voltages at the converter terminals and is only used by the DVC Stateflow block during the start-up procedure. If the MTdc network voltage is above 0.9pu, or 630V, VSC2 and VSC3 are connected to their ac network, one after the other, following a five seconds delay between them.
The last input *Pref* signal -- corresponds to the converters active power set-point established by the system operator. In this implementation, only the active power of VSC2 can be established. This is due to the fact that VSC3 is controlling its active power according to the

offshore wind farm power output, coming from the OPAL-RT real-time simulator, and VSC1 is taken as the MTdc network slack node, compensating for the total system losses.

5.3.3 DVC Experimental Results

The offshore wind farm implementation and the control strategy implementation were finally combined to obtain the experimental results for the validation of the Distributed Voltage Control method. During the experiment, the three converters assumed different roles i.e:

1. VSC1: this converter is a slack node, meaning it is controlling the MTdc network voltage;
2. VSC2: is also a slack node, and its active power reference is established by the transmission system operator;
3. VSC3: is the offshore wind farm converter and controls the active power.

The active power reference of VSC2, together with the offshore wind power curve of VSC3 were given to the DVC Stateflow algorithm implementation, which then outputted the direct voltage references for converters VSC1 and VSC2. The optimization starts at operation time, t = 25s, to allow time for the initialization of the MTdc network. It then runs between operation time, 25 - 260s, which is five seconds shorter than the offshore wind power curve, to allow time for system shutoff.

During the optimization, the DVC algorithm outputs the voltage references of VSC1 and VSC2 to minimize the losses in the MTdc network, and assure that the active power flow scheduling for VSC2 is fulfilled. The active power and the direct voltage resulting from the DVC strategy validation experiments are displayed in **Figure 27**. The VSC1 was activated at operation time, t = 5s, VSC2 was activated at, t = 10s, VSC3 was activated at t= 15s and it started producing power at t= 25s, when also the MTdc network losses optimization started.

The first thing that is noticeable from the direct voltage measurements (see **Figure 27** (a)), is that VSC1 and VSC2 precisely followed the voltage references given by the DVC algorithm. This is due to the PI regulator action on the direct voltage outer controllers of both converters controlling the MTdc network. Additionally, as soon as the optimization started, the direct voltage of VSC3 was increased close to the higher limit constraint of 1.05pu (or 735V) and, as imposed by the DVC algorithm, it stayed below the higher limit constraint during all operation, with the exception of some ripple and start-up transients.

Figure 27: Experimental measurements from the MTdc network experiments to validate the Distributed Voltage Controller

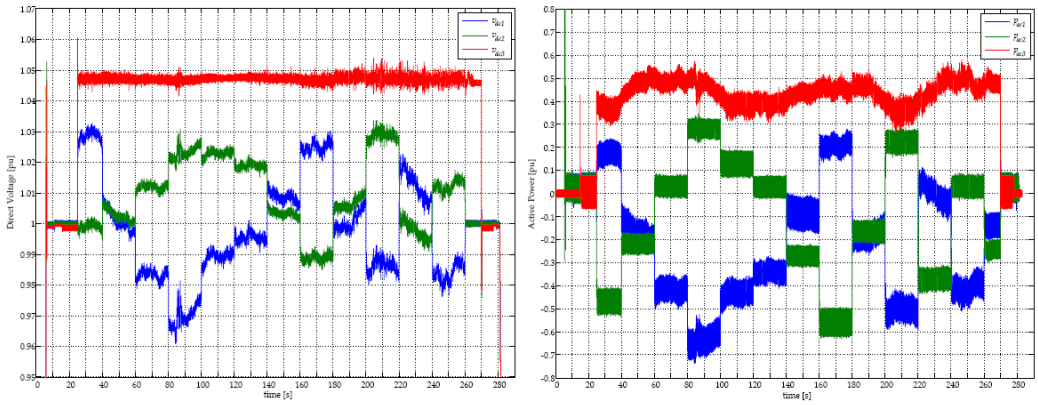

(a) Direct Voltage (b) Active Power

The active power of all three converters during the experiments is shown in **Figure 27**(b). The graphic shows that VSC3 precisely followed the active power curve from the OWEZ wind farm, displayed in **Figure 24**, due to the PI regulator action on its active power outer controller. It is interesting noticing, from the active power graphic, that the active power of VSC2 is unperturbed by the variations in the active power of VSC3. Since VSC1 was chosen as the MTdc network slack node, it absorbs the oscillations in the wind power coming from VSC3, to keep the active power going to VSC2 as close as possible to the established load flow dispatch values.

Finally, the results show that the distributed voltage control strategy is able to successfully operate and control the MTdc network. The complete system had a very good dynamic response, with transients lasting less than 100ms. What is more important, the DVC control strategy has two main advantages: the first is being able to steer the power flow inside the MTdc network according to different optimization goals as stipulated by a transmission system operator. The second, and perhaps most important advantage, is the inherit protection it provides against outages in the converter stations, since more converters are controlling the MTdc network voltage instead of directly controlling their active power.

6

WP5: Optimization

6.1 Transmission Systems Design

Offshore wind farms are increasingly being built further from the coast and in deeper waters. In 2011 the average water depth of offshore wind farms was circa 23 m and the average distance to shore was around 24 km. For under construction projects, the average depth is 25 m, whereas the distance to shore is 33 km. It is believed that this trend will continue in the near future. In this way, it is expected that investment costs of future large offshore wind farms will increase with the longer distances to shore. Therefore, it is important to study and compare the possible transmission technologies in order to reduce investment costs and energy losses as much as possible.

The main objective was to implement a multi-objective approach to compare HVAC and HVDC transmission alternatives. The components of the transmission system were selected from a database which contains real component data and costs.

6.1.1 Optimization Method

In order to apply the MOOA (Multi Objective Optimization Algorithm) to the optimization of the design of offshore transmission systems it is necessary to identify the variables of the problem. In this way, each solution **X** of the algorithm is a vector composed by several variables as follows:

$$\mathbf{X} = \left[\begin{array}{cccc} \alpha & c_1 & \cdots & c_n \end{array} \right]$$

The first field of each solution, α, determines whether **X** represents a HVAC or HVDC transmission system. Every solution holds one variable per component of the respective transmission system. Such variables indicate which components of the database are used. Finally, a variable representing the amount of elements for each component is presented in the chromosomes.

6.1.2 Component Models

In order to optimize the design of offshore transmission systems it is necessary to model every component. **Figure 28** shows the loss curves for AC and DC cables and VSCs that are presented in the database.

Figure 28: Loss curves for AC and DC cables and VSCs

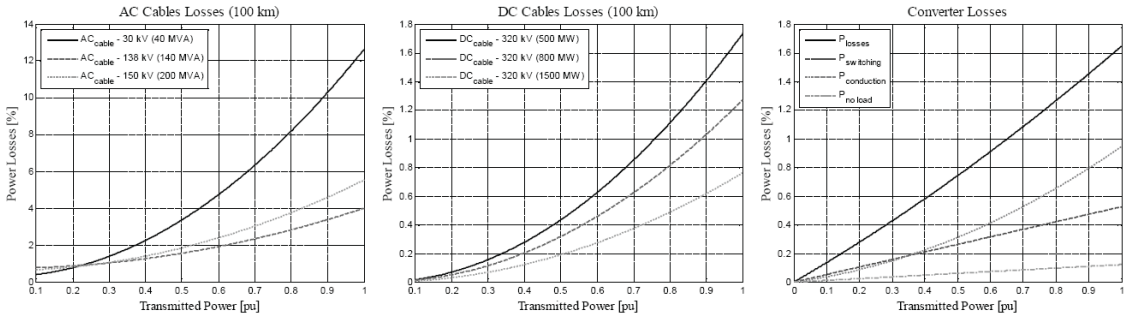

(a) AC Cables (b) DC Cables (c) Converters

6.1.3 Results

When a distance of 50 km is used, as shown in **Figure 29** (a), the AC system is the one that presents the lowest losses and investment costs. Therefore, it is the best option for the transmission system. In **Figure 29** (b), the solutions for a 100 km distance are shown. One of the DC solutions is the one with the lowest energy losses. However, the AC solution presents very similar losses. Moreover, such an AC system is circa three times cheaper compared to the DC system with similar losses. In this way, the AC system is still the best option to connect the offshore wind farm to shore. Finally, when a distance of 150 km is considered, the DC configurations present lower energy losses and total investment costs, when compared to the AC solutions (see **Figure 29** (c)). In this way, for this distance the DC technology is the most advantageous.

Figure 29: Optimal Pareto Fronts for both transmission technologies when distance of 50, 100 and 150 km are considered

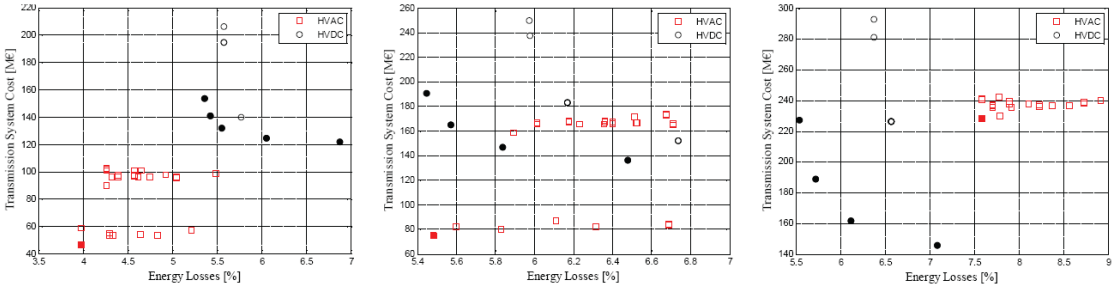

(a) 50 km (b) 100 km (c) 150 km

6.2 MTdc network Power Flow Optimization

There are several reasons contributing to promote the development of an European offshore grid in the North Sea. The main drives are, amongst others, the need to integrate large amounts of renewable energy, the will to boost transnational electricity trade, the European Union's targets on renewable energy generation and desire for security of supply. Several European projects have performed studies on market, regulatory and policy challenges related to the development of a North Sea transnational grid. Nonetheless, hitherto, very few have concentrated on its technical aspects, especially the challenges involved with controlling and operating such networks.
The main objective was to control a multi-terminal dc network (shown in **Figure 30**) having several optimization goals into consideration simultaneously: power losses and social welfare.

Figure 30: The 19 node-meshed connected offshore MTdc network used in the simulations

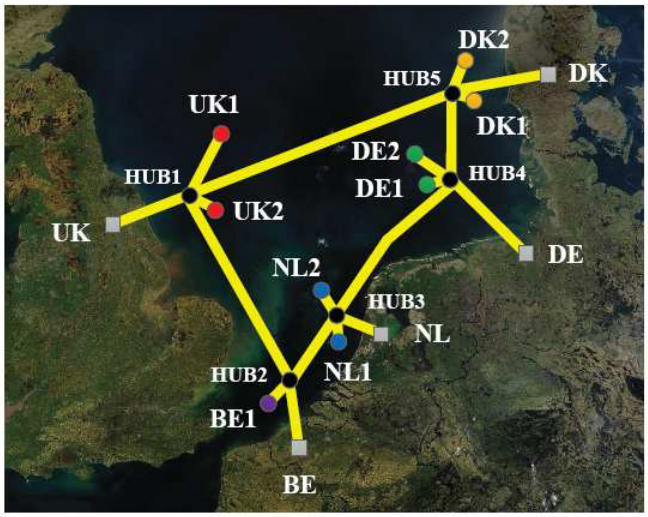

6.2.1 MTdc Control Scheme

All the variables are real valued and the composition of each solution is:

$$\mathbf{X} = \left[\begin{array}{ccc} V^{*}_{DC1} & \cdots & V^{*}_{DCn} \end{array} \right]$$

where V^{*}_{DCn} is the dc system voltage reference of the nth onshore VSC.

In the proposed control method, even when receiving a pre-established amount of power, an onshore VSC station will always be operating as a direct voltage regulating node. However, its voltage reference will be determined by the algorithm after solving the optimal MTdc network load flow.
In order to guarantee that the solutions provided are feasible, several constraints were added to the MOOA. These constraints guarantee that there are no dc cables overloaded, and the dc voltages of all the nodes inside the MTdc grid respect the predefined boundaries,

and the load flow solutions are N-1 secure, i.e. the power control will still be achieved even if an outage occurs in any of the VSC terminals.

6.2.2 Results

Figure 31: Available Pareto front between social welfare and power losses and respective buyers and sellers welfare for the considered case studies

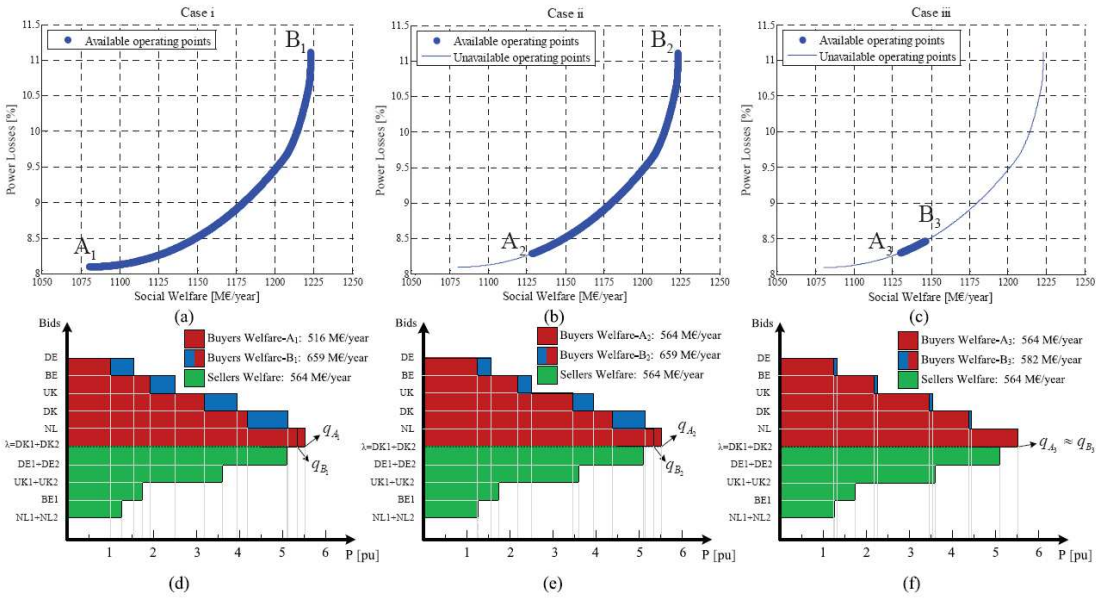

When the N-1 network security constraint is active, the best found Pareto front is shifted towards lower social welfare and higher transmission losses values. To make the dc network N-1 secure, as the maximum dc voltage value is set to 1.15 pu, the algorithm has to lower the onshore dc voltage references -- this explains the higher losses -- because when there is a fault in an onshore node, the dc voltages inside the grid will rise. On the other hand, the social welfare values are lowered since, to maintain network security while optimizing social welfare, less power goes to onshore nodes with higher prices. For instance, when maximum social welfare is considered, the power going to the highest bid, Germany, is reduced from 2.19 pu to 1.55 pu if the MTdc network is N-1 secure. The power balancing among onshore nodes, when N-1 security is considered, happens so that in case of a fault, the offshore power can be shifted to converter stations neighboring the defective one. This step in the optimization process guarantees that, in case of a fault, the converter stations will not be overloaded.

Differently from the maximum direct voltage limitation, the 1-pu current limit in the dc cables hubs demonstrated to be an inactive constraint. For the non-secure MTdc scenario, the maximum hub current was 0.50 pu from HUB3 to HUB4, at the maximum social welfare operating point. For the N-1 secure case, the same situation was encountered but now in the dc cable connecting HUB2 to HUB3. This feature from the algorithm can help the system operator to optimize the hubs installed capacity, and saving costs.

6.3 Conclusions

Transmission Systems Design

The implemented MOOA was able to find feasible solutions for the proposed problem. Optimal Pareto Fronts were achieved for both AC and DC transmission options when different transmission distances were considered. The decision maker can then be presented with these results for the transmission system; and based on the trade-off between the two goals, it will be possible for him to decide which configuration better suits the purposes of the project.

It is important to refer that data from real components was used. Nevertheless, as with any database, the one used is limited in information. Therefore, the results obtained with the algorithm have the database as a major drawback. Moreover, the multi-objective algorithm itself does not guarantee the optimal set of solutions.

MTdc Control: Multi-Objective

Several studies have suggested the construction of a transnational multi-terminal dc network for the interconnection of offshore wind farms, specially in the North Sea. However, optimal power flow control in MTdc networks is still a challenge. In this work, an independent system operator (ISO), which controls the MTdc network via a market pool structure, has been proposed. The introduced ISO is responsible for receiving the pool market participants bids and, after solving an optimal dc power flow, sending the dc voltage references for the onshore converters so that the optimal flow can be realized. The optimization of the MTdc network power flow was performed by a multi-objective genetic algorithm set to optimize the network transmission losses and social welfare. Additionally, a loss allocation procedure was implemented to distribute the transmission power losses costs in a fair way amongst the generator and consumer entities. Through this procedure, market participants with higher power supply and demand were allocated with higher power losses coefficients.

The results from the obtained Pareto fronts indicate the maximum social welfare is achieved when more power is transmitted to countries with higher bids, however, this leads to an increase in transmission losses. Adding extra constraints to the power flow, prohibits the operation in some of the Pareto front regions. Consequently, it may not be possible for the ISO to operate the MTdc network where the best possible cases are found. In this way, the ISO has to decide which is the best operating point for the offshore grid.

The proposed approach to control MTdc network offers a high flexibility to the ISO in obtaining optimal trade-offs. Although, in this work only the transmission losses and social welfare were analyzed, more optimization goals may be considered simultaneously.

7

WP6.1 & 2: Planning and Operation of Offshore Grids & Stability impacts

7.1 Planning and Operation of Offshore Grids

7.1.1 Introduction

In this work package, the consequences of the potential development of a transnational offshore grid in the North Sea on the onshore power system are investigated with the help of market simulations and load flow calculations. This report section is based on Chapter 5 of the PhD thesis of A. Ciupuliga, with supporting methodology for performing the round-the-year security analysis from Chapter 3. As a starting point, a Base Scenario for North-Western Europe in the year 2030 is developed where a high penetration of renewable energy sources (wind and solar) is considered and no transnational offshore grid exists, except for some point-to-point links between countries in the North Sea which are taken into account. These interconnection capacities are kept at their anticipated 2020 values based on the ENTSO-e Ten Year Network Development Plan (TYNDP). For the 2030 scenario, the total amounts of wind power installed are assumed to be: 130.4 GW onshore and 118.8 GW offshore, out of which 52.5 GW are connected to a transnational offshore grid.

7.1.2 Methodology

Detailed chronological and correlated wind power and solar power time series were developed. The market simulation (unit commitment and economic dispatch considering inter-area transmission constraints) is run for the Base Scenario which shows that a high percentage of the wind energy can be integrated, but still considerable amounts of wind energy have to be curtailed. In order to arrive at realistic results, the countries considered in the market model extend beyond the North Sea region as shown in **Figure 32**, covering Belgium, Denmark, France, Germany, Great Britain, Netherlands, Norway and Sweden.

Figure 32: *Transmission corridors in North-Western Europe*

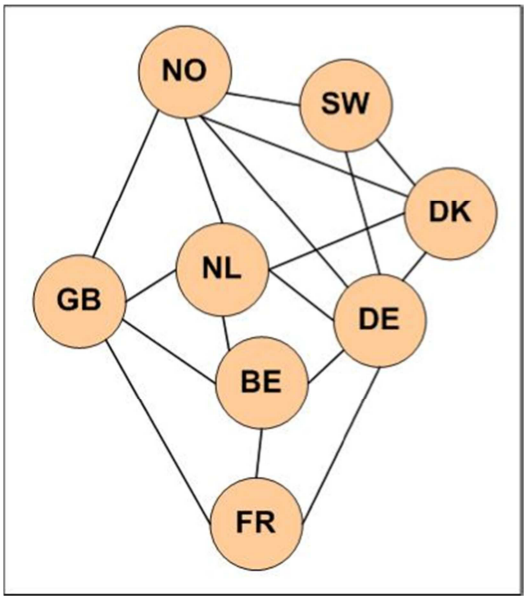

For the market simulations the commercially available PowrSym4 tool was used. The market model is an optimization that considers sequential hourly time steps (within each weekly horizon), with the purpose of obtaining the minimum operating cost (including fuel, emission and start-up costs) at the system level while the technical constraints for generating units and interconnection capacities are met at all times. **Table 6** shows a selection of results for the Base Scenario market simulation.

Table 6: Base *Scenario: main market simulation results*

Pumped Storage Load	[TWh]	25
Curtailed Wind Energy	[TWh]	115
Dump Energy	[TWh]	1.35
Energy Not Served	[TWh]	0.6
CO_2 Emissions	[kton]	345676
CO_2 Cost	[M€]	15900
Fuel Cost	[M€]	30522.1
Start-up Cost	[M€]	2202
Operation & Maintenance Cost	[M€]	6798
Energy Not Served Cost	[M€]	130
Total System Operating Cost	[M€]	55553

It can be noticed that the wasted wind energy (because of system and interconnection

constraints) sums up to 115 TWh, representing 14.7% of the total available wind energy of 781.3 TWh. Besides wasting of wind power, there are still some flexibility problems in the system as there 1.35 TWh of dump energy and 0.6 TWh of energy not served. This means that the system – even though able to integrate almost all available renewable energy – still faces some operational problems due to inflexible generating units and transmission constraints. Note that solar power time series are also developed for France (13 GW) and Germany (66 GW, the government's target for 2030), which impose additional flexibility requirements on the power system. It can be noticed that all point-to-point HVDC offshore links have quite high usages, all of them being more than 80% of the time used and more than 50% of the time used at maximum capacity. This is an indication that additional interconnection capacity within the North Sea might be beneficial.

This WP applies the method introduced in [Ciupuliga et al. 2012] to analyse the security of a mixed offshore-onshore grid with a large penetration of wind energy. The analysis is divided into two parts: one focusing on the offshore grid and one focusing on the offshore grid's impacts on the onshore grid.

In the offshore grid analysis, both market and grid issues are considered for analysing different offshore grid topologies. With the help of zonal market simulations the market benefits of having an offshore grid are assessed. With the help of round-the-year load flow calculations the security of the grid for various combinations of load and generation coming from the market simulation is assessed. In this work only security during N situation was tested, considering that it is still an open question whether an offshore grid should be N-1 secure in itself. A good approach would be to adjust onshore system reserves to loss of individual offshore grid circuits, and at the same time to use reasonable circuit capacities. The round-the-year security analysis is used for estimating how much offshore grid capacity can be given to the market safely. Three different offshore grid topologies were studied: radial, looped and meshed topologies, as shown in **Figure 33**.

Figure 33: : *Investigated offshore grid topologies*

(a) Radial offshore grid topology

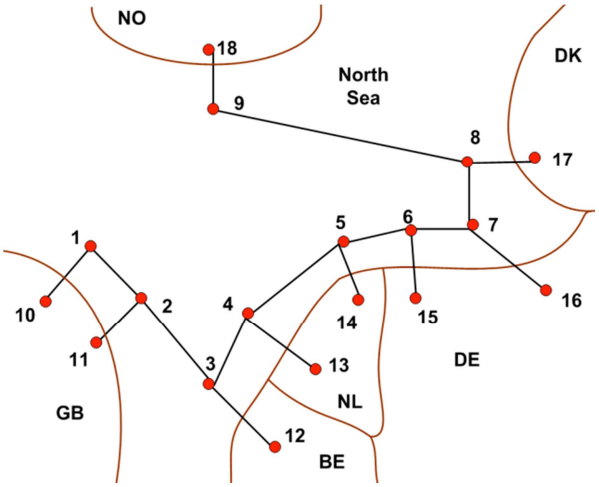

(b) Looped offshore grid topology

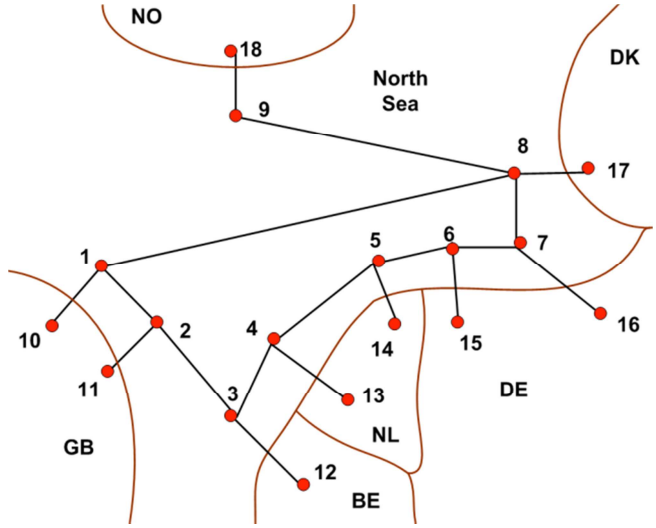

(c) Meshed offshore grid topology

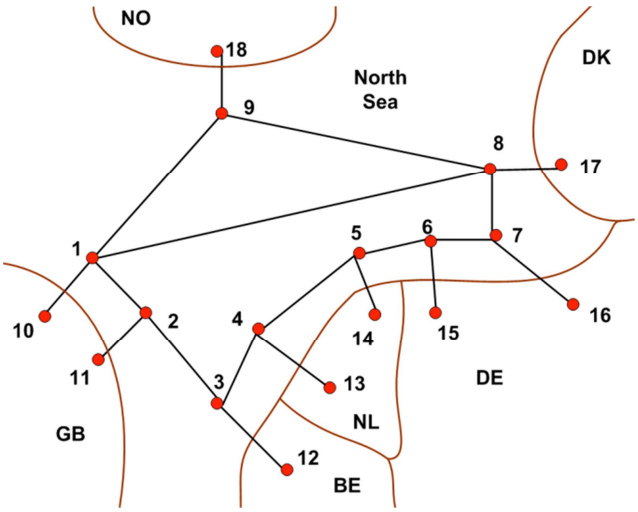

7.1.3 Results

In the analysis performed, grid security, grid utilization factors, operating cost and wind curtailment were considered separately. The results of the market simulations indicate the benefits (e.g. less operating costs, less CO2 emissions, less curtailed wind) of increased interconnection capacity in the North Sea. However, the results show that the usage of links between hubs belonging to the same country is rather low, as those hubs are connected to the same market area. The round-the-year security analysis reveals that with the increase of loops in the offshore grid, less of the grid capacity can be given "safely" (i.e. without resulting in overloads during operation) to the market. Offshore transmission capacity can be better utilized in radial grid structures. As the three investigated grid structures are far from optimal, a more suitable offshore grid structure is proposed, which is both secure and has good utilization factors. This grid structure is shown in **Figure 34**.

Figure 34: *Chosen offshore grid configuration*

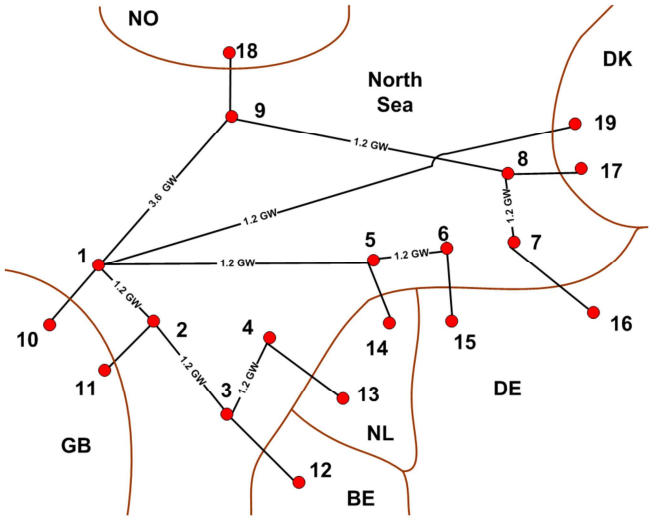

Table 7: *Market simulation results for the chosen offshore grid configuration: usage of the hub-to-hub and hub-to-foreign shore links*

Parameter	Line								
	L1-9	**L1-2**	**L2-3**	**L3-4**	**L5-6**	**L7-8**	**L8-9**	**L1-19**	**L1-5**
Mean power [MW]	2145	398	796	486	321	650	717	743	690
% hours used	75.2	62.1	87.0	67.0	52.3	68.2	68.9	83.4	75.3
% hours at NTC	45.9	6.6	45.6	13.2	17.3	34.9	50.6	45.9	38.8
% hours > 0.5NTC	59.3	31.3	66.0	39.8	23.9	55.4	59.4	60.7	57.2

The offshore grid hub-to-hub and hub-to-foreign shore link usage statistics resulting from the market simulation with the chosen grid topology shown in **Figure 34** are given in **Table 7**. Note that link 1-9 consists of three parallel circuits. All other hub-to-hub links have only

one circuit of 1200 MW.

Once the offshore grid structure is settled upon, the onshore grid analysis investigates the effects of the designed offshore grid on the EHV onshore grid of the Netherlands. To this purpose a detailed 2020 grid model of the Dutch EHV system and simplified models of the Belgian and German EHV systems are used. The planned North-South HVDC corridors in Germany for the year 2032 are modelled in a simplified manner with nodal injection/withdrawal of power. All these constitute the Reference Scenario. Also two reinforcement variants are considered that aim at reducing bottlenecks arising from integrating large-scale wind from the North Sea.. Loadings of selected branches in normal and contingency situations are determined using the commercial software PSS/E version 32. An AC-DC contingency analysis is adopted, for the N and respectively N-1 situations. The contingency analysis is performed only on the Dutch part of the grid including interconnections to neighbouring grids.

The round-the-year security analysis is performed for N and N-1 situations. The occurring bottlenecks in both interior and border lines of the Dutch grid are emphasized and their risks of overload are calculated. **Figure 35** gives an illustration of the geographical spread of the bottlenecks, based on criteria C12, the number or overloaded hours during N-1 situations.

Figure 35: *Reference Scenario: bottlenecks in the Dutch grid according to C12*

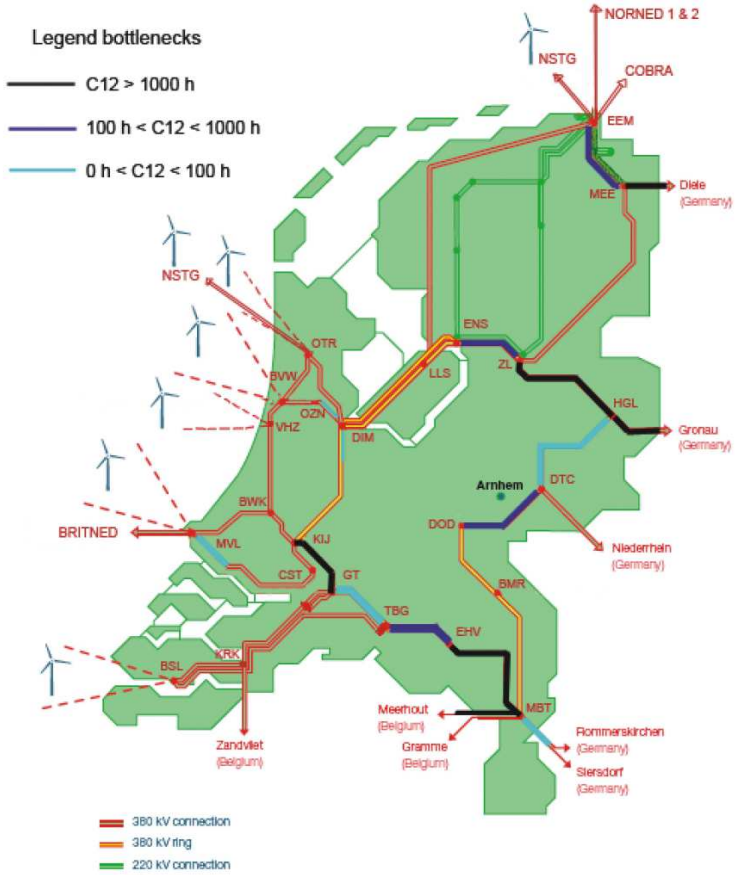

Three main bottleneck areas can be observed, all related to strong power flows on the Northeast-Southeast and Central West-Southeast axes of the Dutch grid. More precisely, there is a trend of high power flows from the Northern and Western wind and

interconnection areas to the load situated more to the South in the German grid. Two reinforcements scenarios are assessed for the interior grid of the Netherlands with some of the TenneT Vision2030 recommendations:

- **Reinf-1**: two circuits are added to the GT-KIJ branch, one circuit is added to the EEM-MEE branch and the capacity of branch HGL-ZL is increased from 1645 MVA to 2633 MVA per circuit.
- **Reinf-2**: the same as Reinf-1, plus a new double circuit branch is added between DIM and DOD, with 2633 MVA per circuit.

Table 8: *Grid risks of overload for the 380 kV NL interior and border grids. Comparison for two reinforcement scenarios*

Grid	Reference Scenario		Reinf_1		Reinf_2	
	$RO_{grid,N}$	$RO_{grid,N-1}$	$RO_{grid,N}$	$RO_{grid,N-1}$	$RO_{grid,N}$	$RO_{grid,N-1}$
	[%*h]					
Interior grid	432.2	126589.2	114	53315	0	5539.8
Border grid	26836.8	104031	27136.2	109835	29485.7	101842.1

Table 8 shows the comparison of the grid risks of overload for the interior grid and for the border grid. It can be noticed that by adding the reinforcements, the internal grid risks of overload are very much reduced as most of the interior bottlenecks can be eliminated/reduced. At the same time the border grid risks of overload are not very much affected as the severity of the border bottlenecks is not significantly changed.

Two sensitivity analyses are further performed with the help of the round-the-year security analysis which gives overall results but also pinpoints critical snapshots for more detailed investigation. The sensitivity analysis to the North-South HVDC corridors in Germany shows that the presence of these corridors is essential for wind integration and reduces the high loop flows through the Dutch grid, and the related overloads. The severity index comparison for the main bottlenecks is illustrated in **Figure 36**(a) and (b). For the interior branches, it can be noticed that not having HVDC corridors in Germany results in much more severe overloads in the Dutch grid for most of the lines, due to more loop flows through the Dutch grid. For the border branches it can be noticed also that in the "No HVDC corridors in DE" scenario the severity of the overloads is higher, especially in the Meeden phase shifter MEE-PST. It is concluded that these corridors are very important for integrating the North Sea offshore wind in the European grid. Consequently, future studies should model these corridors and more accurate models of their operation are needed. It is noticed that it is very important to model accurately the neighbouring systems, and especially the closer parts of these systems have an effect on the results.

In order to understand better, what happens in the grid one snapshot is chosen and a comparison for a critical hour during N situation is performed. The comparison is made for hour 8080 and shown in **Figure 37**(a) and (b) where a qualitative graphical representation of the flows in the Dutch grid is made for both scenarios.

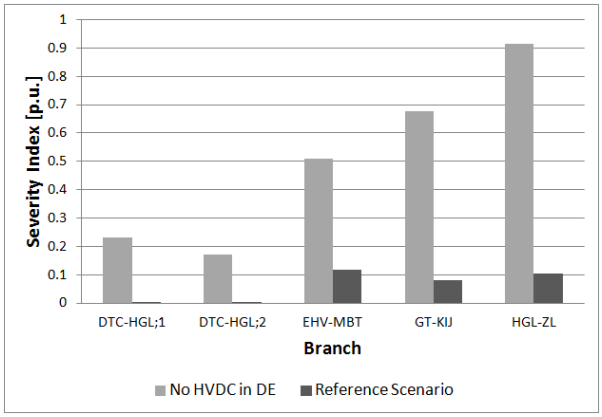

(a) Interior branches

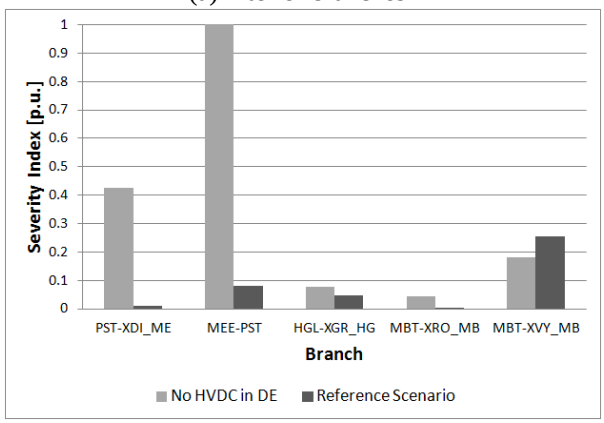

(b) Border branches

Figure 36: *Comparison of main bottlenecks severity indices. Reference Scenario versus Variant Scenario with no HVDC corridors in Germany*

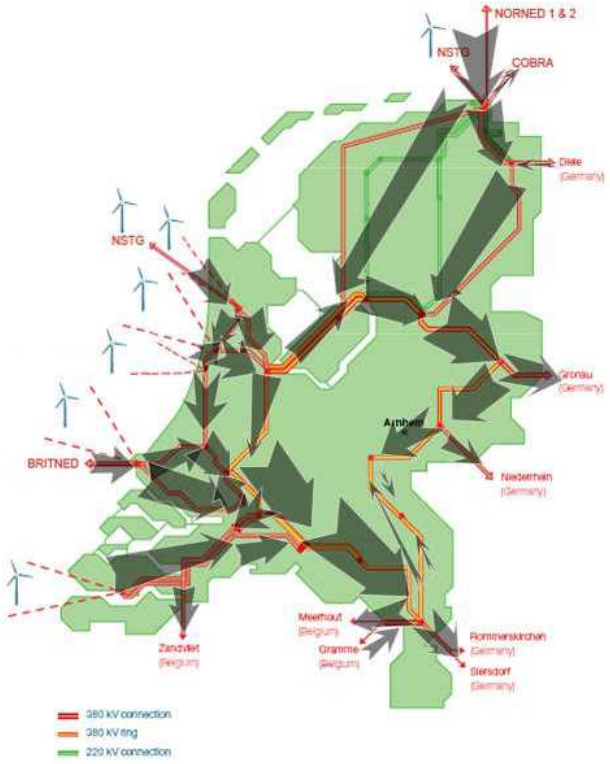

(a): Reference Scenario, HVDC corridors in DE.

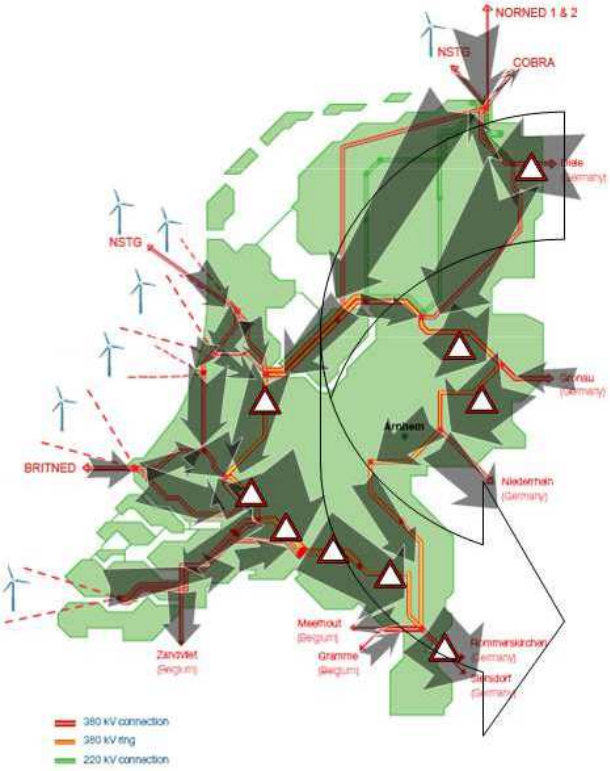

(b): Variant Scenario, No HVDC corridors in DE.

Figure 37: *Power flows in the 380 kV Dutch grid for critical hour 8080, N situation*

This is a high wind hour, with also high imports from the North Sea neighbouring areas. It can be observed that having no HVDC corridors in Germany results in high loop flows through the Netherlands, causing many severe bottlenecks even in the N situation. Approximate 6.7 GW of DE-NL-DE loop flow goes from North to South, creating severe overloads on the cross-border lines but also on the interior lines of the Dutch grid. Because of the highly congested situation in both Dutch and German grids, the adjustment of the phase shifting transformers fails in preventing this loop flow. For the same hour, the presence of HVDC corridors eliminates almost completely the loop flow by sending the power from the North of Germany directly to the load centers in the South of Germany. The influence on the distribution of border flows between the NL and BE can be noticed: when no HVDC corridors exist, more power flows through the Zandvliet border-lines than through the Van Eyck ones.

In the second sensitivity analysis the effects of having a different offshore grid structure or even of not having an offshore grid at all, are investigated. The analysis illustrates that the structure and presence of the offshore grid have a significant influence on the power flows in the onshore grid. The changes in generation dispatch and energy exchanges that come with each sensitivity scenario affect the power flows in the Dutch grid and consequently the bottlenecks and their severity.

7.1.4 Conclusions and Recommendations

Work Package 6.1 focussed on designing a market-adequate and N-secure topology for an offshore grid in the North Sea and on assessing its consequences on the security of the onshore grid, in particular for the Netherlands. It can be concluded that for a robust planning and operation, onshore and offshore grids should be planned together and with consideration of market, operational, control and grid modelling aspects. Assessing the security of a grid has to be done considering many combinations of load and generation. The round-the-year security analysis proved to be very adequate for this, giving a good overall picture of the overloads in the grid.

7.2 Stability impacts

7.2.1 Introduction

Work package (WP) 6 of the NSTG research project addresses the grid integration from a planning, operation, and dynamic behaviour respect. This section addresses the results, conclusions, and recommendations for WP 6.2. The goal of this part of the NSTG research project is to investigate the influence future VSC-HVDC transmission has on dynamics of the interconnected AC system, most notably in the transient stability time-frame of interest (0.1 — 10 s.). It consists of two parts: transient stability assessment and power system oscillation

damping by VSC-HVDC. Both studies were conducted separately, but use the same dynamic models for VSC-HVDC.

Case studies have been performed using a continental European power system model in the software package PSSE, on courtesy of TenneT TSO B.V. VSC-HVDC dynamic models taken from related research projects and WP 3 have been adapted and improved for application into large-scale system studies. Publicly available transmission system models of surrounding (British and Nordic) synchronous areas were adjusted to the time horizon of the NSTG project. Subsequently the influence of several VSC-MTDC topologies, power management methods, and onshore unit commitment schemes on the power system dynamics have been investigated

7.2.2 Scientific Contributions

- VSC model development for stability studies
- HVDC dynamic model development for stability studies
- Simulation speed improvements for HVDC dynamic models by combined simulation methods and multi-rate techniques
- Exploring the efficacy of several power management methods for multi-terminal VSC-HVDC
- Exploration of dynamic (0.1—10 s) interactions between VSC-MTDC and ac systems
- Show how power system oscillations can be damped by VSC-HVDC transmission and indicate which factors influence the effectiveness of this damping
- Wind power plant participation into power oscillation damping.

7.2.3 VSC and Power System Stability

Rotor angle stability concerns the electro-mechanical interactions between rotating equipment during and after faults. It encompasses transient stability and small-signal stability of the power system as shown in **Figure 38**. Despite their excellent controllability VSC-HVDC systems show non-linear and discontinuous behaviour during faults, which must be taken carefully into account in grid integration studies. At present however, HVDC systems as such have little impact on the rotor angle stability of large systems, mainly because current projects are still small-dimensioned. Gradual substitution of conventional generation by renewables, such as VSC-HVDC connected offshore wind power, makes dynamic analysis more and more relevant. As a matter of fact, when future multi-terminal VSC-HVDC systems will connect multiple synchronous areas, it is highly significant to investigate to what extent VSC-HVDC impairs system dynamics

Figure 38: VSC controls couple DC grid dynamics to the rotor angle stability problem

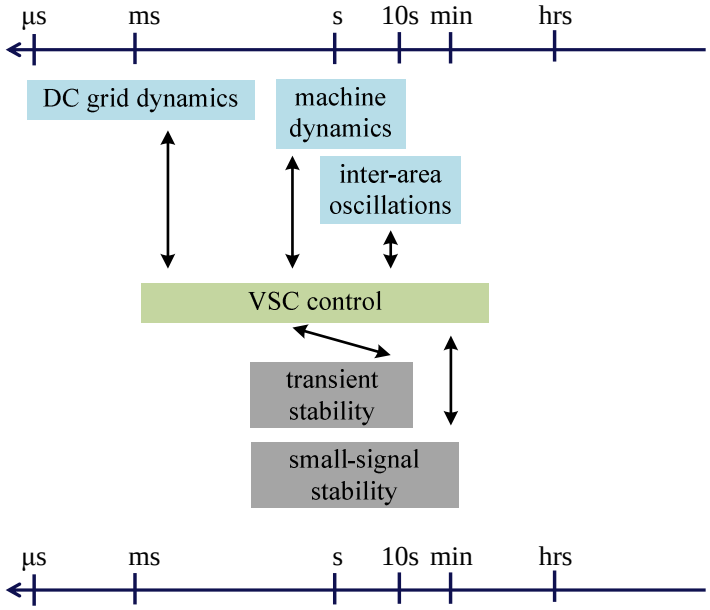

7.2.4 Modelling Assumptions

Offshore WPP Layout

The offshore wind power plant dynamics are only important for the transient stability problem in case the fault-ride through (FRT) implementation requires controlling the offshore VSC and WPP. As in this WP chopper-controlled braking resistors are used as to achieve FRT, the WPPs are aggregately represented by a type IV wind turbine generator with a WPP equivalent power rating, using the PSSE standard models with default dynamic parameters. The aggregated WTG is connected to the offshore VSC by a zero impedance link.

VSC-HVDC Dynamic Modelling for Transient Stability

Power system dynamics in the time-frame of interest for rotor angle stability are traditionally being studied by stability-type simulations. This type of simulation distinguishes itself from others by representing network elements by their 50 Hz equivalent impedance. Quantities such as voltages, currents are represented by quasi-stationary phasors in the time domain. This allows simulation of large-scale AC transmission at reasonable execution speeds.

On one hand, the nature of stability simulations and their corresponding network modelling allows VSCs to be modelled in a simplified fashion, notably the omission of fast controllers and its Norton-equivalent source representation at the AC side. On the other hand, VSC-HVDC transmission shows nonlinear behaviour during faults, most prominently caused by the lack of default overcurrent capability, DC-side voltage balancing logic, and other limiting schemes. A realistic inclusion of these controls requires a detailed representation of the DC-side electromagnetic transients. **Figure 39** shows how this WP implements the VSC and HVDC systems as dynamic models in stability simulations.

Figure 39: General VSC-HVDC model setup in PSSE. The VSC models are implemented as user-written generator models and the DC grid as an artificial speed governor

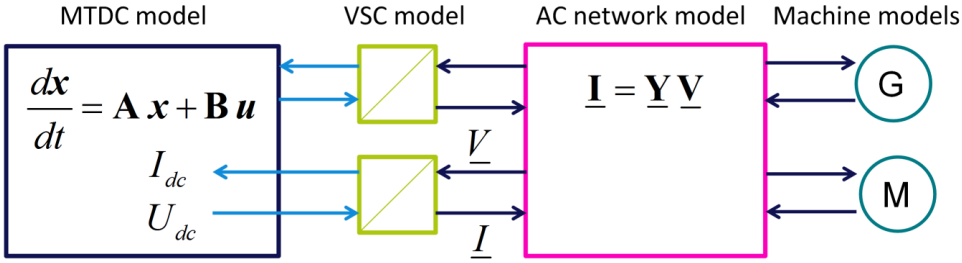

The merit of stability simulations, namely its ability to simulate at with integration step sizes of around half a cycle (**Figure** 40 a), cannot be exploited when also the HVDC system transients should be modelled in detail. The simplest option is to decrease the time-step size for numerical integration into the µs range (**Figure** 40 b). However, this leads to unworkably long simulation times and methods to pertain numerical accuracy and adequate simulation speed should be sought for. In this project, two options were considered to be advantageous: multi-rate simulation in which only the DC dynamic model uses small time-step sizes by inner integration loops (**Figure** 40 c), and combined simulations that use a separate (external) simulation to include the VSC-HVDC system (**Figure** 40 d).

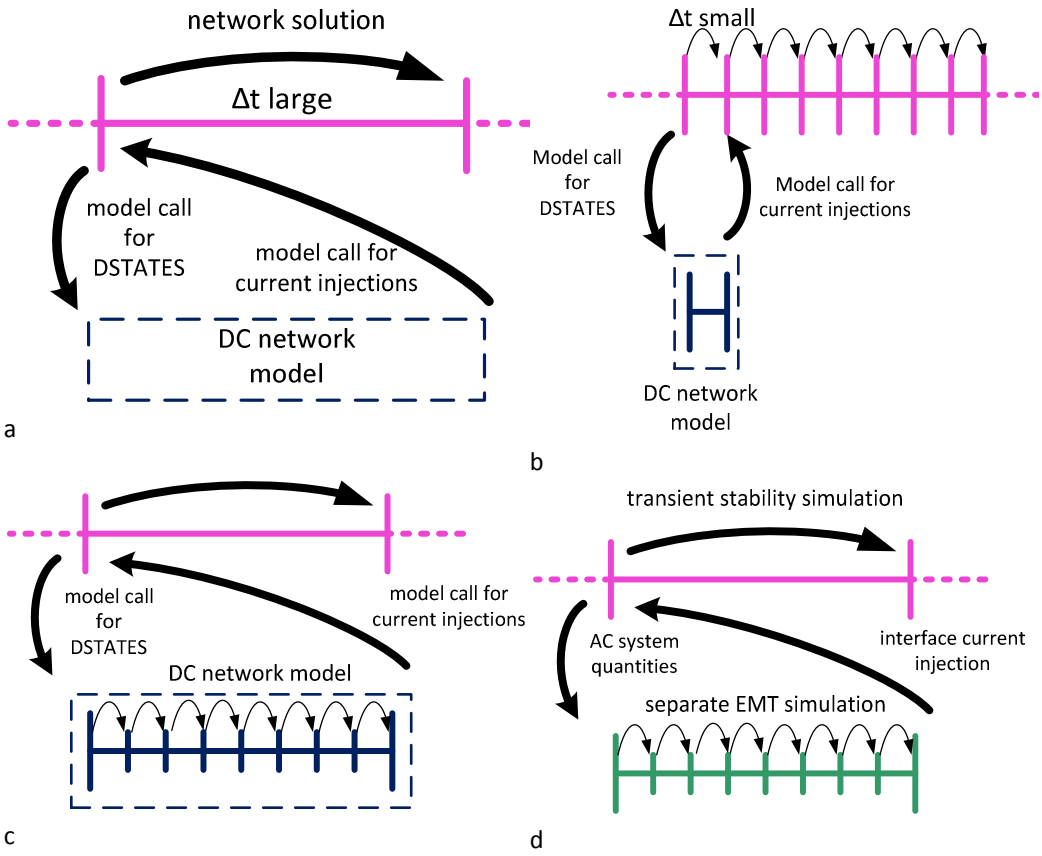

Figure 40: Options for including VSC-HVDC systems in stability-type simulations. a) normal dynamic model, b) decreased time step-size, c) multi-rate implementation, d) co-simulation

The Continental European system model was available in PSSE only, which puts a constraint on the options to use an external simulation for the VSC-HVDC model. Therefore, this WP uses multi-rate techniques to maintain workable execution times.

7.2.5 System Studies

Transmission System Models

The Continental AC dynamic model basically consists of a relatively detailed (20 kV up to 380 kV) Dutch dynamic model based on the 2010 transmission system layout, and a 380 kV transmission system of Belgium, Germany, and France. Adjacent countries are implemented by dynamic equivalent generators. All generators in the dynamic model have appropriate excitation and speed governing systems. The model is particularly developed for the transient stability time-frame of interest and does not contain the European inter-area oscillations properly, which makes is less suitable for small-signal stability studies.

Onshore wind power was modelled for the Netherlands only, with a wind generation fleet amounting to a total of 6 GW. One particular high-wind, low load scenario was considered for the Netherlands. This unit commitment entails 4000 MW of conventional generation, and 14000 MW load. **Table** 9 shows the relevant import to and export from the Dutch transmission network.

Table 9: Import to (Blue) and export from (red) the Netherlands

Belgium	Germany	United Kingdom	Norway
1474	3750	1000	700

The reduced-order dynamic model of the Nordic power system comprises an equivalent benchmark model of 36 buses which is composed of 20 large generators which represent each area in the Nordic system. The system contains both the 0.29 Hz and the 0.55 Hz inter-area modes. The British power system equivalent contains an 8-node, 6-load and 7-generator power system which represents a benchmark model of the UK 380kV transmission system. The 0.5 Hz inter-area oscillation between the Scottish and southern British system is properly included.

NSTG Topologies

The time-horizon of the NSTG project envisages an integration of offshore wind power amounting to a total of 35 GW. All wind power plants are assumed to be connected entirely through VSC-HVDC transmission. In order to investigate the AC-system dynamic behaviour in relation to the offshore grid topology, WP 6.2 assumes two NSTG topologies, as shown in **Figure 41** an option that integrated all offshore wind power by single VSC-HVDC links while no transnational VSC-HVDC connections exist, and an option that interconnects all offshore wind power plants through multi-terminal VSC-HVDC. The latter is in accordance with the “radial” topology used in WP 6.1. All wind park-to-shore connections (cables and onshore VSCs) are rated according to nearest wind power plant rating.

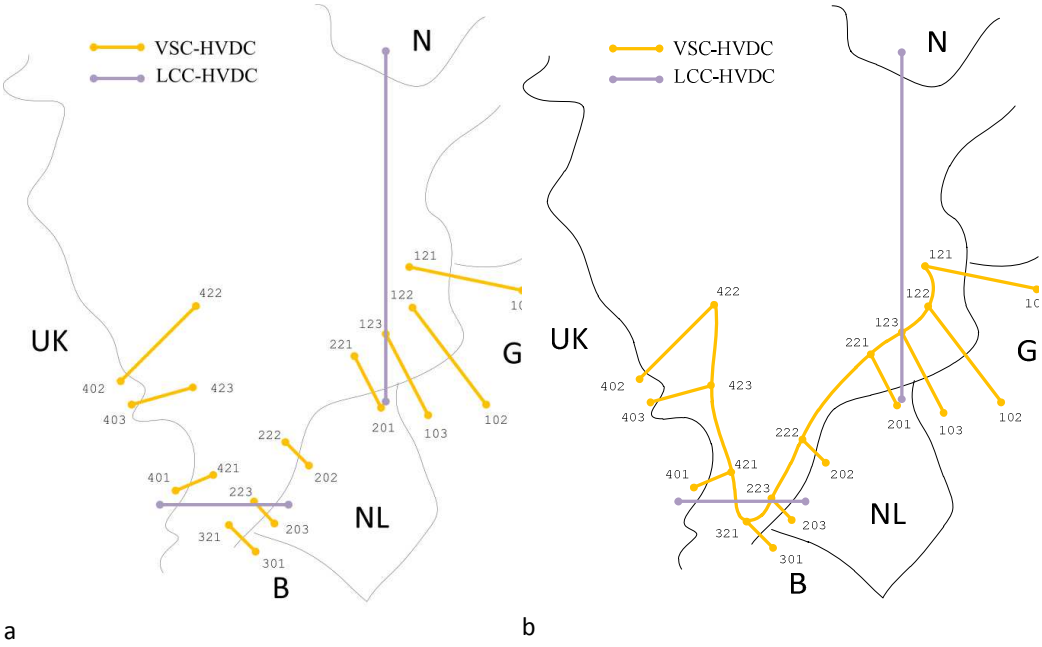

Figure 41: NSTG topologies used for transient stability analysis. a) VSC-HVDC links only, b) U-shaped radial NSTG

Combined AC/VSC-MTDC Power System Dynamics

The integrated AC/VSC-MTDC system was tested under several disturbances, among which short circuits in the Dutch transmission system, remote faults, and wind power plant disconnections. In spite of the extremity of the investigated unit commitment, the large-scale integration of VSC-HVDC showed still plausible generator dynamics throughout the Dutch power system.

To test the influence of several offshore grid control strategies, this WP implemented three types of power management control, namely:

1. All converters control the direct voltage according to a common system direct-voltage droop line.
2. All UK VSCs are in fixed power control mode, and therefore do not participate in compensating imbalances that might appear in the VSC-HVDC system as a result of disturbance events.
3. Each country has a single droop-controlled VSC, which tries to balance voltage fluctuations. The remaining VSCs are in fixed-power control.

Figure 42 shows the G7 rotor speed deviation in the UK system in relation to the abovementioned control methods. An important conclusion that can be gathered from this case is that VSCs that use direct voltage variations to control the power convey the according oscillations into the connected AC system as well. Power system oscillations are thereby propagated from one synchronous area to the second.

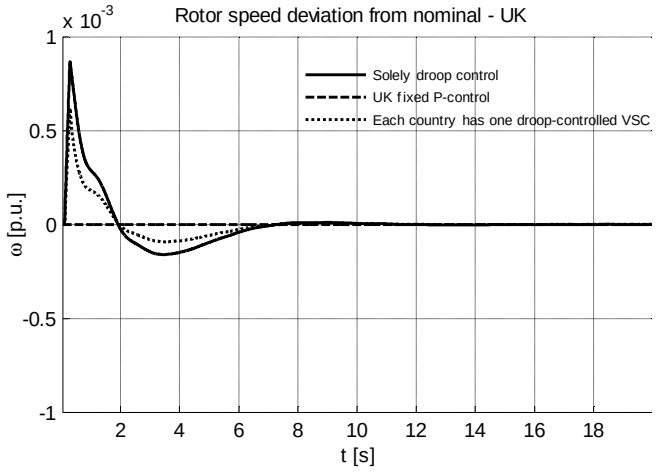

Figure 42: Speed deviation from nominal after a wind power plant disconnection

Transient Stability Assessment

In WP 6.2, critical clearing times (CCT) have been calculated by considering the time-domain simulation results for several fault durations. **Table** 10 shows the CCTs for three-phase short circuits at the terminals 20 kV terminals of the Eemshaven and Borssele generators. The CCTs have been calculated with an accuracy of 5 ms. Higher accuracy would be unrealistic as the fault is cleared per phase in practice whereas the used dynamic model does not allow inclusion of this asymmetry. Slight differences between the U-shaped NSTG and point-to-point links can be observed, in favour of the latter. This could be explained by the propagation of faults through the DC system, but no strict conclusions can be associated with this. Switching the VSCs from continuous voltage control to fixed reactive power control did not show any noticeable effect.

	Eemshaven	Borssele
U-shaped	340	295
Point-to-point	345	310

Table 10: Critical clearing times for the investigated DC grid topologies and selected generators.

Damping Power System Oscillations by VSC-MTDC

After inspection, the available continental system did not show the known inter-area modes. It was considered too inaccurate to draw any significant conclusions in terms of small-signal stability of the Dutch system. However, the inter-area modes of the UK and Nordic system are properly present in the used benchmark systems. Therefore, the scheme shown in **Figure 43** was used to test the power oscillation damping capabilities of multi-terminal VSC-HVDC. The DC grid has a star-shaped topology, with a total wind power integration of 800 MW.

The power oscillation damping (POD) system uses line power flows as an input; its implementation is shown in **Figure** 44 a. Three particular situations have been studied:

1. No POD by any VSC in the network. This was the reference case.
2. The POD is in operation at GSVSC5 in the British system;

3. In order to improve the DC voltage variations (and hence undesired propagation of dynamics), the POD signal is also sent to the active power controller of one of the offshore wind power plants. Ideal—undelayed—telecommunication is assumed.

Figure 44 b shows an exemplary system response using the first two implementations. It can be seen that rotor oscillations are damped accordingly at the expense of direct voltage oscillations (**Figure** 44 c), which propagate to connected synchronous areas. **Figure** 44 d shows that this effect can be mitigated by letting the offshore wind power plants contribute to POD in the British system.

Figure 43: Benchmark system used for testing power oscillation damping

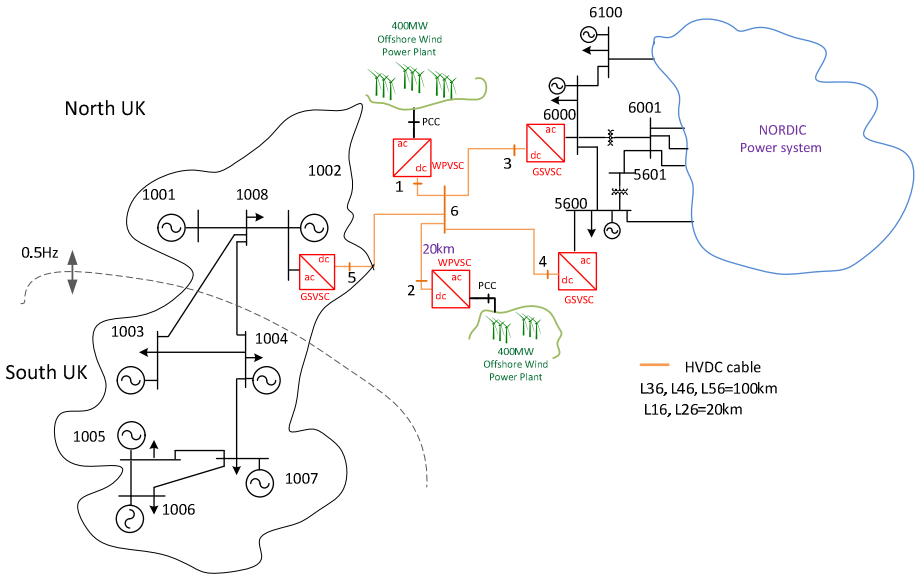

7.2.6 Conclusions and Recommendations

Transient stability assessment

As transient stability software was primarily designed for (large-scale) AC systems, the incorporation of VSC-HVDC structures is non-trivial. Several methods to enhance simulation speed and accuracy have been explored during the course of the NSTG research project, among which modelling simplifications, combined simulations, and multi-rate techniques. This resulted in a dynamic VSC-HVDC model in PSSE that uses inner integration loops to ensure workable execution times.

The transient stability study focussed on the implementation of (a U-shaped) North Sea transnational grid structure as is proposed by WP2 into the existing UK and continental European grid models, notably an adjusted dynamic model that was at the disposal of TU Delft from TenneT TSO B.V. under non-disclosure agreements. Several case studies on the interconnected network model were performed, with the following goals:

1. Show the system time-domain response after test disturbances
2. Show the differences between several offshore grid topologies in terms of power system dynamics
3. Assess critical clearing times for a couple of generators and quantify the influence of the NSTG topology

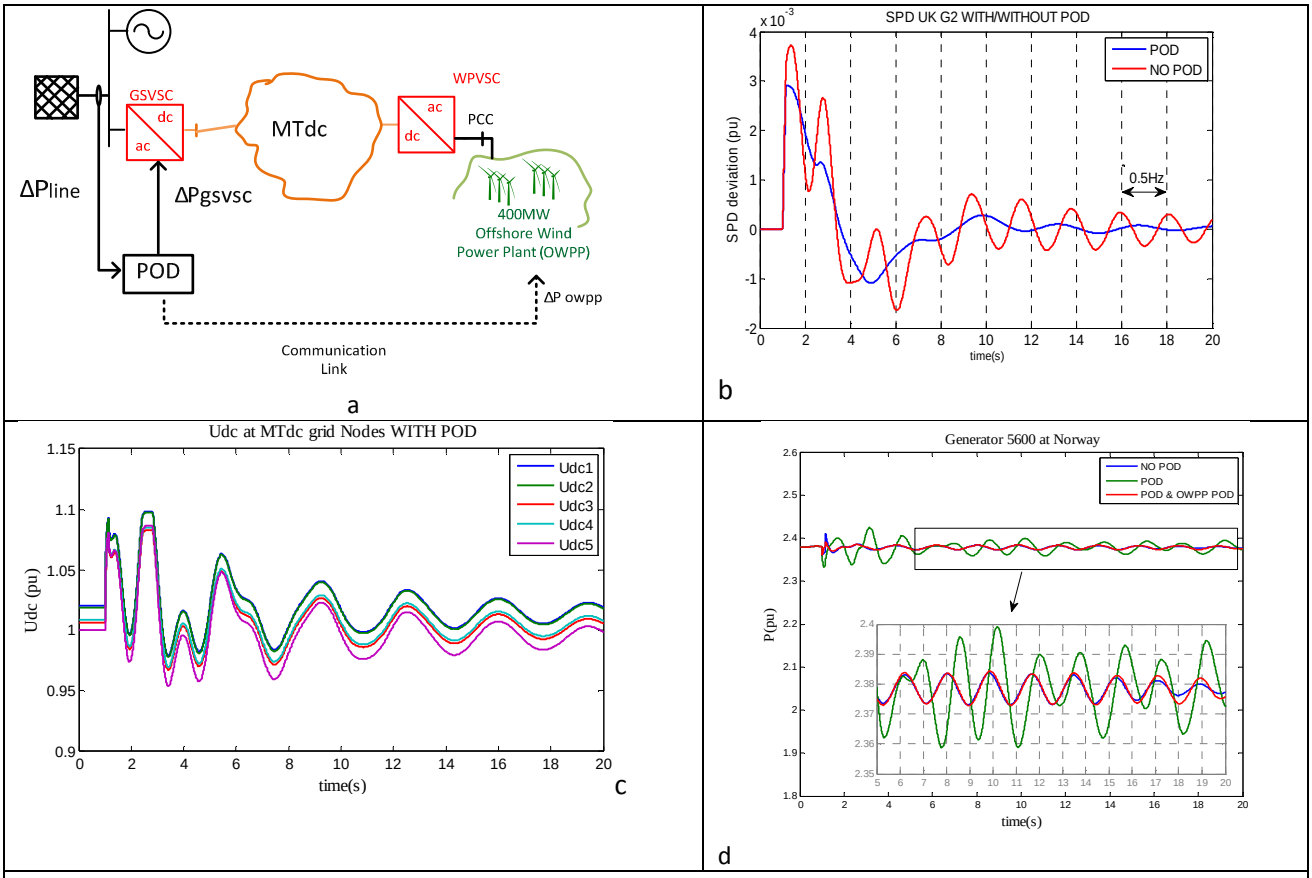

Figure 44: Power oscillation damping by onshore VSCs. a) implementation, b) rotor oscillations in the British system with and without POD, c) direct voltage variations when applying POD, d) dynamics propagation through the NSTG into the Norwegian system.

It was shown that short circuits in one synchronous area are propagated not only to other VSC landing points in the same synchronous area, but also to asynchronous areas, in this case from the Continental system to the UK. Changing the applied power dispatching technique may improve or compound system dynamics in these cases. It was also shown that rotor oscillations are less prominent when operating the DC grid transnationally. However, more investigation is necessary to make this conclusion stronger.

The CCTs for two generation locations have been calculated, both for a U-shaped NSTG and point-to-point links. The differences observed are very small and lie too close to each other to draw any significant conclusions.

Power oscillation damping by VSC-HVDC

Power oscillation damping (POD) is an ancillary service that can be implemented by VSC-HVDC transmission. The applicability of POD for multi-terminal VSC-HVDC schemes was explored in WP 6.2, in which POD method previously applied in literature were taken as a starting point, consequently adjusted for correct interoperability with offshore wind power plant, and tested on an integrated AC/VSC-HVDC power system resembling the northern North-Sea area.

The UK power system illustrates a critical power oscillation mode of 0.5Hz. The hypothesis proved in this report is that this lightly damped oscillation can be damped out effectively by the GSVSC station connected next the North-Scotland equivalent generator. This has been shown via time domain simulations. The damping of the 0.5 Hz (North-South) UK system mode is achieved in short time without jeopardizing the local modes or driving particular modes related to unstable oscillations.

However, the downside of this type of POD in general is that damping oscillations are propagated through the DC system from one synchronous area to the second. This unwanted dynamic coupling should be minimized, and can be resolved by establishing coordination between the GSVSC and the offshore wind power plants through telecommunication links. What is more, it engages offshore wind power plants to participate in the damping of onshore power system by use of their rotor-blades inertia, which in the case of VSC-MTDC networks is fully de-coupled from the ac system.

Recommendations

The applied DC grid control strategy influences system dynamics after the fault. This effect has been quantified but not intensively studied. The main question is whether it is from a control perspective possible to completely isolate the dynamics of the considered asynchronous areas from each other, in most practical situations. Yet, further research efforts should be made in follow-up research projects to back the conclusions drawn on this. The same applies to the conducted CCT analysis.

To achieve this, it is recommended to extend the current study by including the western Danish transmission system and to insert more detailed stability models of the British and Nordic power systems.

The problem of propagation of inter-area oscillation modes through (multi-terminal) VSC-HVDC transmission can be overcome by letting offshore wind power plants contribute to the energy swings involved. This technique puts a heavy burden on fast and reliable telecommunication links. The role of telecommunication in this closed-loop approach should be investigated more elaborately. Moreover, the POD study implemented in WP 6.2 did not take electro-mechanical constraints (e.g. drive-train torsional modes) of offshore wind turbines into account, which could in practice limit the applicability.

Another aspect that was not thoroughly addressed in this research project and which may become an issue when implementing POD on an NSTG, is that inter-area oscillations by definition cause frequency variations across the AC systems. The corresponding phase shift measured by the onshore VSCs should be taken into consideration as well, which extends POD design beyond a mere wind power plant. Therefore, it is advised to focus future research regarding POD on multi-terminal aspects. A more accurate (in terms of small-signal stability) Continental European system that reproduces the known inter-area modes is required in this context.

8

WP7: Costs, benefits, regulations and market aspects North Sea Transnational Grid

This report focuses on the costs and benefits and related policy aspects of a future North Sea Transnational Grid (NSTG). The project studies the effects of a possible future situation in which offshore wind farms in the six NSTG countries: UK, Norway, Denmark, Germany, The Netherlands and Belgium are connected to the nearest shore but also to each other through a future offshore ring. A major source of benefits to society of the additional interconnection capacity of an offshore grid relates to the fact that in the presence of the envisaged North Sea Transnational Grid, a larger share of electricity generation will take place where generation costs are lowest. For a number of scenarios for demand, generation and transmission capacities, these benefits have been quantified by simulations, using the European electricity market model COMPETES.

An offshore ring structure, connecting offshore wind farms from different countries, is one of the key factors distinguishing the NSTG project from other studies involving integration of offshore wind farms and interconnectors. With most offshore wind farms located further from the coast, DC cables would be more appropriate than AC connections. In that case, the additional investment costs of a North Sea ring infrastructure is primarily due to the cost of the required cables.

TSOs developing interconnector projects are faced with more cost items for interconnection than just converters and cables, such as project management and surveys. For the cost-benefit comparison in this work package it has therefore been assumed that for the total scenario costs for the cost-benefit analysis, 10% will be added to the cost parameters for converter stations and cables as reported in the EeFarm database. For the investment costs of the offshore ring a value of 1.47 M€/km will be used with an uncertainty of [-15%,+25%].

Including this 10% on top of the EeFarm cost data brings the resulting specific cost figure used in the middle of a range of a number of public sources analysed in the framework of this project [1.27-1.63 M€/km]. Using this input, the additional investment costs of the 1200 MW ring infrastructure are estimated to be about €3.3 billion.

The impact of a transmission project is assessed by comparing different scenarios with and without the considered ring infrastructure. Each scenario involves generation optimization for given levels of electricity demand and installed generation capacities.
Total benefits of one scenario compared to another have been computed as the relative increase in benefits for the transmission capacity owners (the increase in congestion rent) plus the benefits for the producers (the increase in the producer surplus) plus the reduction in the electricity bill of the consumers. When these annual benefits are discounted with a discount rate of 5.5% and the costs are subtracted, what remains is the Net Present Value (NPV). When projects of similar scale are compared, the higher the NPV, the more beneficial the project is for the investor or society at large, depending on whose costs and whose benefits are compared. A negative NPV implies that the best decision is not to implement the project at all.

Three alternative scenarios have been analysed. One without an offshore ring, in which all the offshore wind farms are only connected to the shore (the No Ring scenario). In the second, or project scenario, an additional ring structure is connecting the offshore wind farms with each other, besides their connections to shore (the Full Ring scenario). The third scenario considers an additional onshore ring, with some offshore sections the (Full Ring Equivalent).

The main output of the scenario analysis at the most aggregated level is provided in Table 1. Shown is the difference between the Net Present Value of the two scenarios with a ring structure compared to the baseline situation without an offshore ring. These are provided for the six countries which are supposed to invest in the North Sea Transmission Grid (The NSTG countries UK, Norway, Denmark, Germany, the Netherlands and Belgium), for the other European countries and for all European countries combined .

Table 11: The difference in Net Present Value of two NSTG scenarios (Full Ring and Full Ring Equivalent) compared to the No Ring scenario assuming that benefits will be gained over a lifetime of 30 years (in billion $€_{2010}$)

NSTG scenarios	NSTG countries	Other countries	EU28 + 7 countries
Full Ring	-1.76	3.46	1.69
Full Ring Equivalent	-2.29	3.61	1.33

From the table it can be concluded that net benefits for the whole of Europe are higher in a Full Ring scenario than in the Full Ring Equivalent scenario. Furthermore, from the viewpoint of social welfare in the NSTG countries only, both investment options are not beneficial since there is a loss to society when compared to net benefits accrued in the No Ring scenario.

The difference in the net benefits between the No Ring scenario and the Full Ring scenario per country is shown in **Figure 45**. An important observation that becomes immediately clear from looking at this figure and the previous table is that net benefits do not necessarily end up in the investing countries, but also in surrounding countries that do not pay but will free-ride (e.g. France). This also applies the other way around since Spain, a country that is not one of the NSTG project countries, will encounter lower total net benefits when a Full Ring offshore grid will be constructed.

Figure 45: Difference in the net benefits between the No Ring scenario and the Full Ring scenario per country assuming that benefits will be gained over a lifetime of 30 years (in billion $euro_{2010}$)[1]

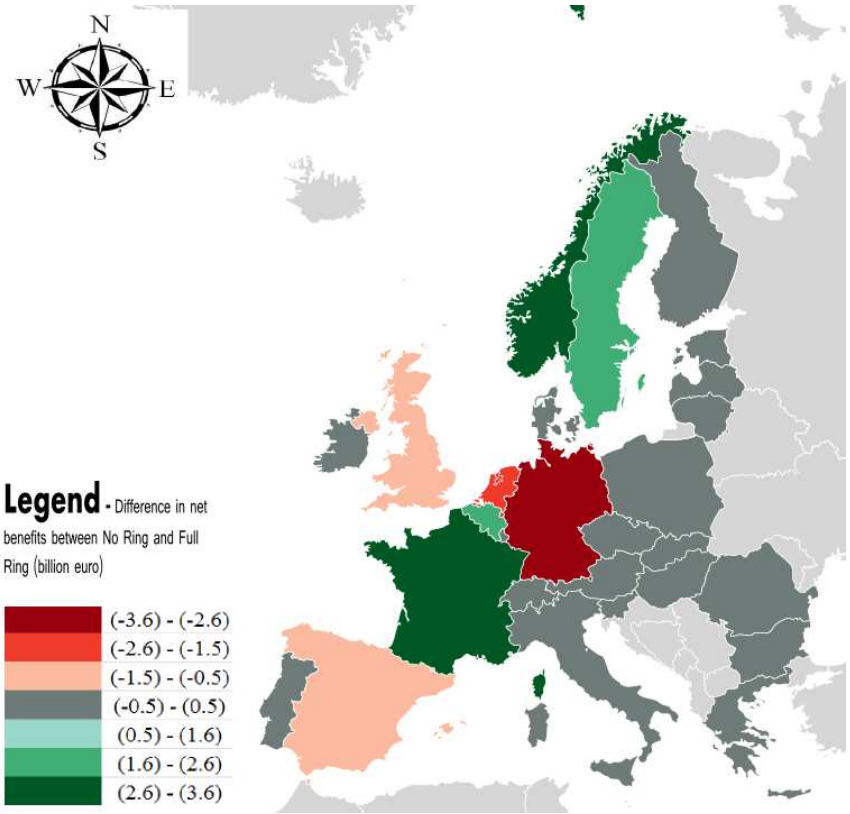

The following conclusions can be drawn:

1. For Europe as a whole (i.e. EU28+7), both the investments in the offshore ring and the mainly onshore Full Ring Equivalent would be beneficial since both have a positive NPV compared to the situation in which offshore wind farms are only connected to the nearest shore (as shown in the last column of table 1).
2. For Europe as a whole, an offshore ring is slightly more beneficial than a parallel ring with an equivalent capacity which is mainly onshore (Full Ring Equivalent). However, the differences in NPV between these two ring scenarios are relatively small (only €0.36 billion) compared to the total investment cost in the ring, which amounts to about €3.3 billion. From an economic point of view, there is therefore only a small preference for an offshore

[1] Investment costs of the full ring are divided over the NSTG countries in proportion to the offshore wind installed NSTG capacity.

ring over an equivalent onshore ring. However, the difference in net benefits to society of these two alternatives is too small to be able to conclude on a clear preference for one over the other.

3. When all offshore ring costs would be born by just the six NSTG countries bordering the North Sea, adding an offshore ring structure to the wind farm connections is not beneficial for the NSTG countries, as is shown by the negative NPV values in the first column of Table 13. This conclusion is valid for both ring scenarios.

4. Free-rider effects caused by profiting from the benefits, but at the same time not having to bear the costs, makes both ring structures beneficial for the group of non-NSTG countries. This finding is not affected by the location of the ring (onshore or offshore): both ring scenarios show positive NPV values for the non-NSTG countries.

The latter two findings are crucial for the viability of a future North Sea Grid. A solution needs to be found in which part of the costs of an offshore grid are allocated to those countries outside the NSTG countries that will benefit from it. Under the assumptions used here, this would require an annual transfer in the order of magnitude of about €240 million per year from non-NSTG countries to NSTG countries. Additional transfers will be required to compensate those non-NSTG countries which will be negatively affected, such as for example Spain. The current ITC mechanism within ENTSO-E, which is meant to compensate TSOs for effects on third countries, is limited to only €100 million per year for the whole of Europe. This is absolutely insufficient to make an offshore grid viable for the NSTG countries. A North Sea grid is therefore unlikely to take off until the ITC mechanism has been improved and strengthened substantially.

For the NSTG countries combined, it would not be beneficial to implement an offshore grid in the absence of an improved ITC mechanism. An alternative cost allocation mechanism that is only valid within the group of NSTG countries would not be sufficient to overcome this barrier without an appropriate ENTSO-E wide ITC mechanism.

Another obstacle for setting up a transnational grid connecting off shore wind is that current national support schemes only cover offshore wind generation fed into the national grid. Yet another major barrier is the lack of a suitable mechanism to compensate TSOs for the consequences of facilitating the transfer of power between two other countries. Due to an annual cap, the current ENTSO-E organised Inter TSO Compensation (ITC) mechanism is completely insufficient to cover the large financial transfers required from non-NSTG countries that benefit from the investments in the NSTG countries.

It can be concluded that integration of offshore wind into an offshore grid will potentially save costs compared to a mainly onshore alternative. However, the large existing regulatory barriers make it unlikely that a North Sea Transnational Grid can be realised in the coming decade.

Advisory Group and International Collaboration (IEA Annex 25)

On 12 and 13 october 2009 an IEA Annex 25 workshop was organized at ECN. The IEA Annex 25 workshop on 16-17 march 2010 in Toledo was visited by TUD EPS. TUD EPS contributed to the IEA Annex 25 workshop in Montreal (October 2010) and attended the IEA Annex 25 meeting in Lisbon in September 2011.

The first Advisory Group meeting was organised at Schiphol on 16 June 2010. The second Advisory Group meeting was organised at Schiphol airport on August 29 2011.

NSTG Reports, Papers, and Website

WP2:
North Sea Transnational Grid: NSTG Wind farm locations and development (WP2)
J.T.G. Pierik
ECN-E–10-072, ECN, 2010

North Sea Transnational Grid - Evaluation of NSTG options (WP2)
J.T.G. Pierik
ECN-E-14-003, ECN 2014

WP3:
Dynamic wind farm model for North Sea Transnational Grid:
Description of Wind farm and converter concepts for NSTG
NSTG WP3
E.J. Wiggelinkhuizen
J.T.G. Pierik
ECN-E–14-xxx, ECN 2014

WP3 and 4:
Multi – Terminal DC Networks: System Integration, Dynamics and Control
Rodrigo Teixeira Pinto
PhD Thesis, TU Delft, January 2014

WP5:
North Sea Transnational Grid: Work Package 5 - Optimization of North Sea Transnational Grid solutions
Silvio Rodrigues, Pavol Bauer, Edwin Wiggelinkhuizen and Jan Pierik
TU Delft, October, 2013

WP6.1:
Transmission Extension Planning under Increased Uncertainties

Ana Roxana Ciupuliga
PhD Thesis, TU Delft, October 2013

WP6.2:
Damping Of Power System Oscillations by VSC-HVDC Multi-Terminal Transmission Networks
WP 6.2. NSTG Project Technical Report, Part I
Mario Ndreko, Arjen van der Meer, Barry Rawn and Madeleine Gibescu
TU Delft 2013

Dynamic Behaviour and Transient Stability Assessment of a North-Sea Region Case Containing VSC-HVDC Transmission
A. A. van der Meer, M. Ndreko, B. G. Rawn, M. Gibescu
WP 6.2. NSTG Project Technical Report, Part II
TU Delft, 2013

WP7:
Cost, benefits, regulations and policy aspects of a North Sea Transnational Grid
F.D.J. Nieuwenhout
M. van Hout
December 2013
ECN-E--13-065

NSTG papers per work package:

WP 3 and 4:

Journals

1. R. Teixeira Pinto, S. F. Rodrigues, P. Bauer, and J. Pierik, “Description and Comparison of DC Voltage Control Strategies for Offshore MTDC Networks: Steady-State and Fault Analysis,” European Power Electronics Journal, vol. 22, no. 4, pp. 13 - 21, 2013.

2. R. Teixeira Pinto, P. Bauer, S. Rodrigues, E. Wiggelinkhuizen, J. Pierik, and B. Ferreira, “A Novel Distributed Direct-Voltage Control Strategy for Grid Integration of Offshore Wind Energy Systems Through MTDC Network,” IEEE Transactions on Industrial Electronics, vol. 60, no. 6, pp. 2429 -2441, June 2013.

3. R. Teixeira Pinto, S. F. Rodrigues, E. Wiggelinkhuizen, R. Scherrer, P. Bauer, and J. Pierik, “Operation and Power Flow Control of Multi-Terminal DC Networks for Grid Integration of Offshore Wind Farms Using Genetic Algorithms,” Energies, vol. 6, no. 1, pp. 1-26, 2012. [Online]. Available: http://www.mdpi.com/1996-1073/6/1/1

4. S. Rodrigues, R. Teixeira Pinto, P. Bauer, and J. Pierik, “Optimal Power Flow Control of VSC-based Multi-Terminal DC Network for Offshore Wind Integration in the North Sea,” IEEE Journal of Emerging and Selected Topics in Power Electronics - Early Access, vol. PP, no. 99, pp. 1-9, 2013. [Online]. Available: http://ieeexplore.ieee.org/arnumber=6600728

5. E. Kontos, R. Teixeira Pinto, S. F. Rodrigues, and P. Bauer, “Impact of HVDC Transmission System Topology on Multi-Terminal DC Network Faults,” Submitted to IEEE Transactions on Energy Delivery on October 14th 2013, vol. PP, pp. 1-8, 2013.

Conferences

1. A. van der Meer, R. Teixeira Pinto, M. Gibescu, P. Bauer, J. Pierik, F. Nieuwenhout, R. Hendriks, W. Kling, and G. van Kuik, “Offshore Transnational Grids in Europe: the North Sea Transnational Grid Research Project In Relation To Other Research Initiatives,” Proceedings of the 9th International Workshop on Large-Scale Integration of Wind Power Into Power Systems As Well As On Transmission Networks For Offshore Wind Power Plants, Quebec, Canada, October 2010.

2. R. Teixeira Pinto and P. Bauer, “Modular Dynamic Models of Large Offshore Multi-Terminal DC (MTDC) Networks,” Proceedings of the European Wind Energy Association Conference, Brussels, Belgium, March 2011, pp. 1-10.

3. R. Teixeira Pinto and P. Bauer, “The Role of Modularity Inside the North Sea Transnational Grid Project: Modular Concepts for the Construction and Operation of Large Offshore Grids,” Proceedings of the Renewable Energy World Europe Conference, Milan, Italy, June 2011, pp. 1-19.

4. R. Teixeira Pinto, S. Rodrigues, P. Bauer, and J. Pierik, “Comparison of direct voltage control methods of multi-terminal DC (MTDC) networks through modular dynamic models,” in Proceedings of the 2011-14th European Conference on Power Electronics and Applications (EPE 2011), Birmingham, England, 30 2011-sept. 1 2011, pp. 1 -10.

5. S. Rodrigues, R. Teixeira Pinto, P. Bauer, and J. Pierik, “Optimization of Social Welfare and Transmission Losses in Offshore MTDC Networks Through Multi-Objective Genetic Algorithm,” in 7th International Power Electronics and Motion Control Conference (IPEMC), vol. 2, Harbin, China, June 2012, pp. 1287 -1294.

6. S. Lazarou, E. Wiggelinkhuizen, R. Pinto, P. Minnebo, H. Wilkening, J. Pierik, and G. Fulli, “A Smart Grid Simulation Centre at the Institute for Energy and Transport - Integration of Large Amounts of Offshore Wind Energy,” in Complexity in Engineering (COMPENG), Aachen, Germany, June 2012, pp. 1 -6.

7. S. Rodrigues, R. Teixeira Pinto, P. Bauer, E. Wiggelinkhuizen, and J. Pierik, “Optimal power flow of VSC-based multi-terminal DC networks using genetic algorithm optimization,” in IEEE Energy Conversion Congress and Exposition (ECCE), Raleigh, USA, sept. 2012, pp. 1453 -1460.

8. R. Teixeira Pinto, S. F. Rodrigues, P. Bauer, and J. Pierik, “Optimal Control Tuning of Grid Connected Voltage Source Converters using a Multi-Objective Genetic Algorithm,” in Proceedings of the Power Conversion Intelligent Motion (PCIM Europe), Nuremberg, Germany, 14 - 16 May 2013, pp. 1 -8.

9. R. Teixeira Pinto, S. F. Rodrigues, P. Bauer, and J. Pierik, “Control and Operation of a Multi-terminal DC Network,” in 8th International Power Electronics and Motion Control Conference (IPEMC), Melbourne, Australia, June 2013, pp. 1 - 8.

10. S. F. Rodrigues, R. Teixeira Pinto, P. Bauer, and J. Pierik, “Multi-Objective Optimization of a PMSG Control System through Small-Signal Analysis,” in 8th International Power Electronics and Motion Control Conference (IPEMC), Melbourne, Australia, June 2013, pp. 1 - 8.

11. B. Elizondo, R. Teixeira Pinto, and P. Bauer, “Sustainable DC-Microgrid Control System for Electric-Vehicle Charging Stations,” in Proceedings of the 2013-15th European Conference on Power Electronics and Applications (EPE 2013), Lille, France, sept. 2013, pp. 1 -10.

12. M. Sieragakis, R. Teixeira Pinto, and P. Bauer, “Control of an 80-kW Wind Turbine Connected to a DC Microgrid,” in Proceedings of the 2013-15th European Conference on Power Electronics and Applications (EPE 2013), Lille, France, sept. 2013, pp. 1 -10.

13. R. Teixeira Pinto, S. F. Rodrigues, P. Bauer, and J. Pierik, “Grid Code Compliance of VSC-HVDC in Offshore Multi-terminal DC Networks,” in IECON 2013 - 39th Annual Conference on IEEE Industrial Electronics Society, Vienna, Austria, July 2013, pp. 1 - 5.

WP 5:
Comparison of Offshore Power Transmission Technologies: a Multi-Objective Optimization Approach. Silvio Rodrigues, Graduate Student Member, IEEE, Pavol Bauer, Senior Member, IEEE and Jan Pierik. YR Symposium Delft 2012.

Optimization of Social Welfare and Transmission Losses in Offshore MTDC Networks through Multi-Objective Genetic Algorithm. Silvio Rodrigues, Graduate Student Member, IEEE, Rodrigo Teixeira Pinto, Graduate Student Member, IEEE, Pavol Bauer, Senior Member, IEEE and Jan Pierik . Presented at ECCE 2012 China

WP 6.1:
A. R. Ciupuliga, E. Pelgrum, M. Gibescu, M. A. M. M. van der Meijden, and W. L. Kling. A Market-Based Investigation of Large-Scale Renewable Energy Integration in Northwestern Europe. Accepted for IEEE PES GM 2012, 22-26 July 2012, San Diego, USA.

WP 6.2:
"Offshore Transnational Grids in Europe: The North Sea Transnational Grid Research Project in Relation to Other Research Initiatives"
Arjen A. van der Meer, Rodrigo Teixeira Pinto, Madeleine Gibescu, Pavol Bauer, Jan T. G. Pierik, Frans D. J. Nieuwenhout, Ralph L. Hendriks, Wil L. Kling, Gijs A. M. van Kuik

A.A. van der Meer, R. L. Hendriks, M. Gibescu, W. L. Kling: Interfacing Methods for Combined Stability and Electro-magnetic Transient Simulations applied to VSC-HVDC, accepted for IPST 2011, Delft.

"Control of Multi-Terminal VSC-HVDC for Wind Power Integration Using the Voltage-Margin Method". Christian Ismunandar, Arjen A. van der Meer, Madeleine Gibescu, Ralph L. Hendriks, Wil L. Kling

"Combined Stability and Electro-Magnetic Transients Simulation of Offshore Wind Power Connected through Multi-Terminal VSC-HVDC". Arjen A. van der Meer, Graduate Student Member, IEEE, Ralph L. Hendriks, Graduate Student Member, IEEE, and Wil L. Kling, Member, IEEE

A. van der Meer, R. L. Hendriks, M. Gibescu, J. A. Ferreira, M. A. M. M. van der Meijden, and W. L. Kling, "Combined simulation method for improved performance in grid integration studies including multi-terminal VSC-HVDC," in Proc. Renewable Power Generation conference, Edinburgh, United Kingdom, Sep. 6-8, 2011.

L. Bergfjord, A.A. van der Meer, A. R. Ciupuliga, and M. Gibescu. Effects of offshore grid design on multi-area power system operation. In 6th IEEE Young Researchers Symposium in Electrical Power Engineering, Delft, the Netherlands, April 16-17 2012.

P. J. D. Chainho, A. A. van der Meer, R. L. Hendriks, M. Gibescu, and M. A. M. M. van der Meijden. General modeling of multi-terminal vsc-hvdc systems for transient stability studies. In 6th IEEE Young Researchers Symposium in Electrical Power Engineering, Delft, the Netherlands, April 16-17 2012.

A. A. van der Meer, R. L. Hendriks, M. Gibescu, J. A. Ferreira, and W. L. Kling, "Hybrid simulation methods to perform grid integration studies for large scale offshore wind power connected through VSC-HVDC," in Proc. EPE Joint Wind Energy and T & D Chapters Seminar, Trondheim, Norway, May 9-11, 2011.

B. G. Rawn, P. Lehn, M. Maggiore, "A Disturbance Margin For Quantifying Limits on Power Smoothing by Wind Turbines", IEEE Transactions on Control System Technology.

The NSTG reports and the public papers can be downloaded from the NSTG website: www.nstg-project.nl